

FINAL REPORT
CLOSED FLUME INLET EFFICIENCY

FDOT Contract No.: BDK80-977-36

AUTHORS

Marian Muste, Ph.D.

Andrew Craig, M.S., P.E.

IIHR-HYDROSCIENCE & ENGINEERING
The University of Iowa
100 C. Maxwell Stanley Hydraulics Laboratory
Iowa City, IA 52242
(319) 335-5237
iihr@uiowa.edu

M. Emre Bayraktar, Ph.D. (PI)

OHL School of Construction
College of Engineering and Computing
Florida International University
10555 West Flagler St.
Miami, FL 33174
(305) 348-3174
bayrakm@fiu.edu

Submitted to:

Florida Department of Transportation
Research Center
605 Suwannee Street, MS30
Tallahassee, FL 32399

April 2014

DISCLAIMER

The opinions, findings, and conclusions expressed in this publication are those of the authors and not necessarily those of the State of Florida Department of Transportation.

APPROXIMATE CONVERSIONS TO SI UNITS

SYMBOL	WHEN YOU KNOW	MULTIPLY BY	TO FIND	SYMBOL
LENGTH				
in	inches	25.4	millimeters	mm
ft	feet	0.305	meters	m
yd	yards	0.914	meters	m
mi	miles	1.61	kilometers	km

SYMBOL	WHEN YOU KNOW	MULTIPLY BY	TO FIND	SYMBOL
MASS				
oz	ounces	28.35	grams	g
lb	pounds	0.454	kilograms	kg
T	short tons (2000 lb)	0.907	megagrams (or "metric ton")	Mg (or "t")

SYMBOL	WHEN YOU KNOW	MULTIPLY BY	TO FIND	SYMBOL
TEMPERATURE (exact degrees)				
°F	Fahrenheit	$\frac{5}{9} (F-32)$ or $(F-32)/1.8$	Celsius	°C

TECHNICAL REPORT DOCUMENTATION PAGE

1. Report No.	2. Government Accession No.	3. Recipient's Catalog No.	
4. Title and Subtitle Closed Flume Inlet Efficiency		5. Report Date April 2014	
		6. Performing Organization Code	
7. Author(s) Marian Muste, Andrew Craig, and M.E. Bayraktar		8. Performing Organization Report No.	
9. Performing Organization Name and Address OHL School of Construction Florida International University 10555 West Flagler Street, EC 2900 Miami, FL 33174		10. Work Unit No. (TRAIS)	
		11. Contract or Grant No. BDK80-977-36	
12. Sponsoring Agency Name and Address Florida Department of Transportation 605 Suwannee Street Tallahassee, FL 32399		13. Type of Report and Period Covered Final Report September 2012 – May 2014	
		14. Sponsoring Agency Code	
15. Supplementary Notes			
16. Abstract The goal of the present study was to determine the efficiency of a specific culvert geometry, labeled as Index 216 Closed Flume Inlet (CFI) in the FDOT's Design Standards, and to determine if geometric changes affect the efficiency of the current design. The experimental study was initiated by testing the impact of various changes to the Index 216 CFI geometry to determine the optimum configuration with respect to hydraulic operation. The 4-ft unstricted geometry was found to be optimal CFI configuration. Subsequently, extensive series of tests were carried out to estimate the hydraulic performance of this geometry for a wide range of settings and flow conditions. Final empirical relationships to predict the CFI intercepted flow have been developed using analysis and visualization. While there are no references to compare the results obtained in the present study, the hydraulic performance of the tested drainage structures is aligned with the analytical inferences. Moreover, the trends of the results obtained herein are in agreement with results of previous studies conducted on similar drainage structure geometry. Overall, it can be concluded that: (i) increased cross- slopes convey more stormwater through the drainage structure for the same longitudinal slope and (ii) decreased longitudinal slopes convey more flow through the drainage for the same cross-slope. The efficiency of the drainage structures for larger cross-slope is modest while a sharp decrease occurs for larger longitudinal slopes. The assessment of the CFI hydraulic performance also includes the estimation of the self-cleaning velocity. It is observed that the self-cleaning velocity is exceeded for all tested situations.			
17. Key Words: storm drains, drainage structures, curb inlets, shallow flows, pavement hydraulics, close inlet flumes, gutter flows.		18. Distribution Statement No restriction.	
19. Security Classif. (of this report) Unclassified	20. Security Classif. (of this page) Unclassified	21. No. of Pages 78	22. Price

EXECUTIVE SUMMARY

Florida Department of Transportation (FDOT) provides design standards to support the design, construction, and maintenance of the Closed Flume Inlets (CFI) that are used to redirect storm water from the curbs into roadside drainage ditches or swales. In the 1970s, the majority of FDOT inlets were evaluated to determine their hydraulic efficiency. In the 1990s, the CFIs were introduced, and they have not been evaluated for hydraulic efficiency or debris control yet. Following their implementation, multiple pre-cast drainage structure manufacturers have proposed changes to the original CFI design. These changes include unconstricted barrel cross-section, different interior slopes, and different barrel lengths. The goal of the present study was to determine the efficiency of the Index 216 CFI specified by FDOT's Design Standards eBooklet (FDOT, 2014) and to determine if geometric changes affect the efficiency of the current design.

The complexity of the flow through this ubiquitous drainage structure precludes estimation of the hydraulic efficiency using numerical simulations or analytical approaches. The best approach to provide accurate knowledge of the hydraulic behavior for various CFIs is the experimental investigation. The experimental study was initiated by testing the impact of various changes to the Index 216 CFI geometry to determine the optimum configuration with respect to hydraulic operation. The 4-ft unconstricted geometry was found as the optimal CFI configuration. Subsequently, extensive series of tests were carried out to estimate the hydraulic performance of this geometry for a wide range of settings and flow conditions. Final empirical relationships to predict the CFI intercepted flow have been developed using analysis and visualization. These relationships are presented in graphical and tabular forms to facilitate the use of the physical modeling results.

While there are no references to compare the results obtained in the present study, the hydraulic performance of the tested drainage structures is aligned with the analytical inferences. Moreover, the trends of the results obtained herein are in the agreement with results of previous studies conducted on similar drainage structure geometry. Overall, it can be concluded that that:

- increased cross-slopes convey more stormwater through the drainage structure for the same longitudinal slope
- decreased longitudinal slopes convey more flow through the drainage for the same cross-slope.

The efficiency of the drainage structures for larger cross-slope is modest while a sharp decrease occurs for larger longitudinal slopes. The assessment of the CFI hydraulic performance also includes the estimation of the self-cleaning velocity. It is observed that the self-cleaning velocity is exceeded for all tested situations. The present study does not address economical and maintenance factors nor design criteria for the optimum spacing and selection of drainage inlet types of various geometries.

TABLE OF CONTENTS

DISCLAIMER	ii
APPROXIMATE CONVERSIONS TO SI UNITS	iii
TECHNICAL REPORT DOCUMENTATION PAGE	iv
EXECUTIVE SUMMARY	v
LIST OF TABLES	viii
LIST OF FIGURES	ix
<u>CHAPTERS</u>	
1. INTRODUCTION	1
2. BACKGROUND	3
2.1 General Considerations	3
2.2 Preliminary Considerations on Closed-Flume Inlets	5
3. STUDY APPROACH	10
3.1 Study Objectives	10
3.2 Phasing of the Investigation Tasks.....	11
3.3 Modeling Matrix	13
4. EXPERIMENTAL FACILITIES AND PROCEDURES	16
4.1 Scale Selection and Similitude Considerations.....	16
4.2 Test Facilities	17
4.3 Model Construction.....	17
4.4 Flow Conveyance and Measurement	23
4.5 Measurement Protocols	25
5. EXPERIMENTAL RESULTS	26
5.1 Screening Test Results	26
5.2 Performance Test Results.....	34
6. CONCLUSIONS	46
REFERENCES	47
APPENDIX A: Index 216 CFI	49
APPENDIX B: CFI Type 5 and 6	52
APPENDIX C: Numerical Results	57

LIST OF TABLES

Table 1: Modeling scenarios for the screening tests.....	14
Table 2: The longitudinal and cross-section slopes used for the Performance Tests	15
Table 3: Model similitude criteria based on a 1:5 length ratio	16
Table 4: Mean velocity over the CFI for selected low flow cases.....	39
Table C: Numerical results of experiments	57

LIST OF FIGURES

Figure 1: Perspective drawing of inlets	4
Figure 2: Closed flume inlet configurations	6
Figure 3: Gutter flow: S and Sx indicate longitudinal slope and cross-slopes	7
Figure 4: Closed flume inlet	8
Figure 5: CFI efficiency obtained through hydraulic modeling	8
Figure 6: The geometry of the CFI prototype to be investigated in the study	9
Figure 7: Plan and elevation views of CFI model.....	18
Figure 8: Model detail and section views (2% cross-slope shown).....	19
Figure 9: Upstream perspective view of CFI model.....	20
Figure 10: Upstream view of v-notch weir box and model including a close-up of the weir box	21
Figure 11: Rendered photo of the model	22
Figure 12: Photographs of the various parts of the model (final CFI installed)	23
Figure 13: Comparison of output from turbine meter and V-notch weir equation over the full range of flows to be tested.	24
Figure 14: Photos of the downstream CFI cross section used to determine the average cross-sectional velocity	25
Figure 15: Constricted CFI model with D = 4 ft.....	27
Figure 16: Constricted CFI model with D = 5 ft.....	27
Figure 17: Constricted CFI model with D = 6 ft.....	27
Figure 18: Unconstricted CFI model with D = 4 ft.....	27
Figure 19: Side view of the unconstricted CFI model with D = 4 ft and sidewalk inlet	27
Figure 20: The effect of the CFI interior slope screening tests.....	28
Figure 21: The effect of the CFI constriction screening tests.....	30
Figure 22: Screening tests for evaluating the effect of the addition of the 2-ft-long sloping CFI extension	32
Figure 23: Comparison between regression fits applied to the raw experimental data	35
Figure 24: Hydraulic performance for 4-ft, 2% cross-slope CFI.....	36
Figure 25: Hydraulic performance for 4-ft, 3% cross-slope CFI.....	36
Figure 26: Hydraulic performance for 4-ft, 4% cross-slope CFI.....	37
Figure 27: Hydraulic performance for 4-ft, 5% cross-slope CFI (all longitudinal slopes).....	37
Figure 28: Hydraulic performance for 4-ft, 6% cross-slope CFI (all longitudinal slopes).....	38
Figure 29: Hydraulic performance for 4-ft, 0.3% longitudinal slope CFI (all cross-slopes).....	41
Figure 30: Hydraulic performance for 4-ft, 1.0% longitudinal slope CFI (all cross-slopes).....	41

Figure 31: Hydraulic performance for 4-ft, 1.5% longitudinal slope CFI (all cross-slopes).....	42
Figure 32: Hydraulic performance for 4-ft, 3.0% longitudinal slope CFI (all cross-slopes).....	42
Figure 33: Hydraulic performance for 4-ft, 4.0% longitudinal slope CFI (all cross slopes).....	43
Figure 34: Hydraulic performance for 4-ft, 5.0% longitudinal slope CFI (all cross slopes).....	43
Figure 35: Trends in the variation of the maximum and minimum diverted flows with the change in the cross and longitudinal slopes	44
Figure 36: Comparison of the hydraulic performance curve	45
Figure A: FDOT 2014 design standards-closed flume inlet-index 216.....	49
Figure B: FDOT 2014 design standards-curb inlet tops types 5 and 6.....	52

1. INTRODUCTION

The physical modeling study presented in this report verifies the hydraulic performance of the closed flume inlet (CFI) currently deployed by Florida Department of Transportation (FDOT). CFIs are designed and constructed in conformity with the recently reviewed specifications put forth by FDOT (FDOT, 2012; FDOT, 2014). Despite the extensive literature on these inlets for pavement drainage, the hydraulic performance of these drainage structure is widely based on empirical relationships that hold only for which the geometry of the structure and the flow ranges for the relationships were developed. Consequently, the establishment of the hydraulic performance of specialized CFI configurations (such as the ones tested in the present study) is best served by physical modeling.

Experiments reported here were conducted at the IIHR-Hydropscience & Engineering (IIHR), University of Iowa (<http://www.iihr.uiowa.edu>). IIHR has been part of the University of Iowa's central campus since 1920 and currently manages more than 120,000 square feet of floor space dedicated to research, teaching, and research support. The experimental facility and some of the instrumentation used in the study were built in-house using the available expertise and infrastructure. Similar studies were conducted for Iowa Department of Transportation and National Cooperative Highway Research Program.

The results of this experimental study provide FDOT with accurate knowledge of the hydraulic behavior of several types of CFIs over a wide range of flow situations. The current knowledge about the hydraulic capacity of existing CFI designs is obtained from general equations that were obtained experimentally for similar but different geometries. Slight differences in geometry can considerably change the flow pattern through the structure, hence posing some issues with the CFI designers. This study used similitude theory and physical modeling to establish more accurate information that currently cannot be obtained with alternative means (including numerical simulations) as the flow through the CFI is highly three-dimensional, hence complex.

The study results are presented in tabular and graphic form to facilitate the use of the modeling results. Several dependencies were visualized in order to provide a physical understanding of the

role of variables involved in this complex flow. The assessment of the CFI hydraulic performance includes the estimation of the self-cleaning velocity in the model for all flow ranges in order to make sure that clogging does not occur in typical storm flow situations. The study does not address economical and maintenance factors neither design criteria for the optimum spacing and selection of drainage inlet types of various geometries.

The study is presented in the following order. First, a short review of the available literature is summarized. Next, the facilities, instrumentation and operation protocol are described. Subsequently, the results of the screening tests that led to the selection of an optimal CFI configuration are presented and discussed. The last portion of the study presents the hydraulic performance for the selected optimal CFI configuration. Conclusions and recommendations are closing the report.

2. BACKGROUND

2.1 General Considerations

Stormwater drainage systems are designed to collect surface runoff and redirect the runoff to a treatment unit. An efficient stormwater drainage system should quickly remove the runoff from streets, minimize the potential for flooding, and permit the transportation arteries to function during storms. The removal of stormwater from streets is accomplished by collecting the overland flow in gutters and intercepting the gutter flow at inlets. Based on the Federal Highway Administration's Hydraulic Engineering Circular No. 12, inlets used for the drainage of highway surfaces can be divided into three major classes including: **(i)** curb-opening inlets, **(ii)** gutter inlets, and **(iii)** combination inlets.

Each major class has many variations in design and has been well-defined for its functionality with the corresponding hydraulic efficiency (Mays, 2010). Figure-1 illustrates several types of inlets. Curb-opening inlets are vertical openings in the curb covered by a top slab. Gutter inlets include two types of inlets: grate inlets, consisting of an opening in the gutter covered by one or more grates; and slotted inlets, consisting of a pipe cut along the longitudinal axis with a grate of spacer bars to form slot openings. Combination inlets usually consist of both a curb-opening inlet and a grate inlet placed in a side-by-side configuration, but the curb opening may be located upstream of the grate.

The hydraulic capacity of different types of CFIs has been previously investigated experimentally for various conditions (e.g., Conner, 1945; USACE, 1949; Wintz and Kuo, 1969). The CFI performance has been also approached numerically (e.g., Li et al., 1954; Bauer and Woo, 1964) and through direct field measurements (e.g., Anderson, 1972). The flow at these structures is however highly three-dimensional therefore the results of the available studies are confined to a specific geometry of the inlet and its vicinity as well as for the range of flow that were investigated. The complexity of the flow is best simulated at this time by physical modeling whereby use of similitude and appropriate scale model can replicated the flow quite

well. The present study approaches the hydraulic performance of the CFI structure using an experimental approach.

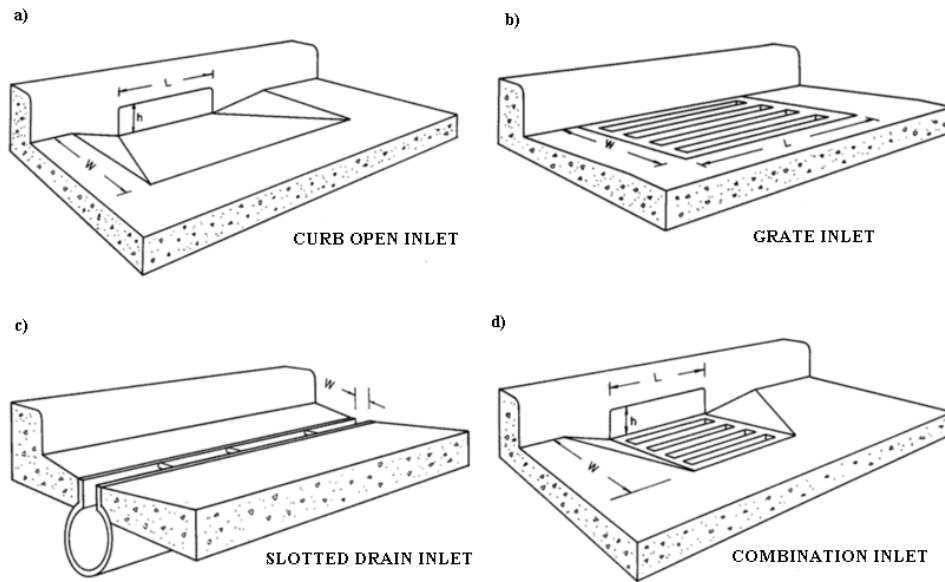


Figure 1: Perspective drawing of inlets

a) curb-opening inlet; b) grate inlet; c) slotted inlet; and d) combination inlet (Mays, 2010)

FDOT uses extensively CFIs to redirect stormwater from the curb and gutter directly into a shallow roadside drainage ditch or swale. FDOT provides theoretical background for design through the Storm Drain Handbook released in 2012 (FDOT, 2012). In addition, the Design Standards eBooklet further supports the design, construction, maintenance, and utility operation's engineering processes for the State Highway System (FDOT, 2014). Index 216 of these design standards, introduced in the 1990s, depicts the design details and criteria for the Closed Flume Inlet (see Appendix A). The design of these culverts is similar to Type 5 curb inlet tops (FDOT, 2014) also illustrated for convenience in Appendix B. The design criteria for this class of inlets is for use with Type F curb and gutter only and is located outside of the curb ramp area in FDOT's Design Standards. CFIs, like culverts, can be designed as a single or multiple-barrel flume depending on the design flow rate. As specified in the Design Standards, the Single Barrel Flume is for moderate flows and the Multiple Barrel Flume is for heavy flows.

The geometry of the CFI is defined in the FDOT Design Standards (FDOT, 2012; FDOT, 2014); however, their hydraulic efficiency and debris control have not been hydraulically evaluated for the range of flow conditions produced by storms. In addition, multiple manufacturers have proposed several changes to the CFI design. Those changes differing from the standards in Index 216 include unstricted flow design (removal of the inlet's taper) for debris control purposes, different inlet opening capacities to improve hydraulic capacity, and different interior slopes to provide self-cleanout of debris from the inlet. The potential impact of such changes on the hydraulic efficiency and debris control of the CFI are within the scope of this study.

2.2 Preliminary Considerations on Closed-Flume Inlets

2.2.1 Closed Flume Inlet Configuration

Figure-2 illustrates the configuration of the Single Barrel Flume for CFI. The main CFI design criterion is to remove accumulated stormwater off the roadway as quickly and efficiently as possible. As mentioned above, Index 216 was introduced in the 1990s and has not been evaluated for hydraulic efficiency or debris control. One of the main objectives of the proposed research is to determine the hydraulic efficiency of the CFI for a range of flows. The evaluation of the hydraulic efficiency will follow the guidelines for other types of FDOT inlets. The CFI hydraulic capacity evaluation can be made using various analytical approaches (e.g., Johnson and Chang, 1984). Alternatively, the CFI efficiency can be evaluated based on modeling studies (e.g., Anderson, 1972).

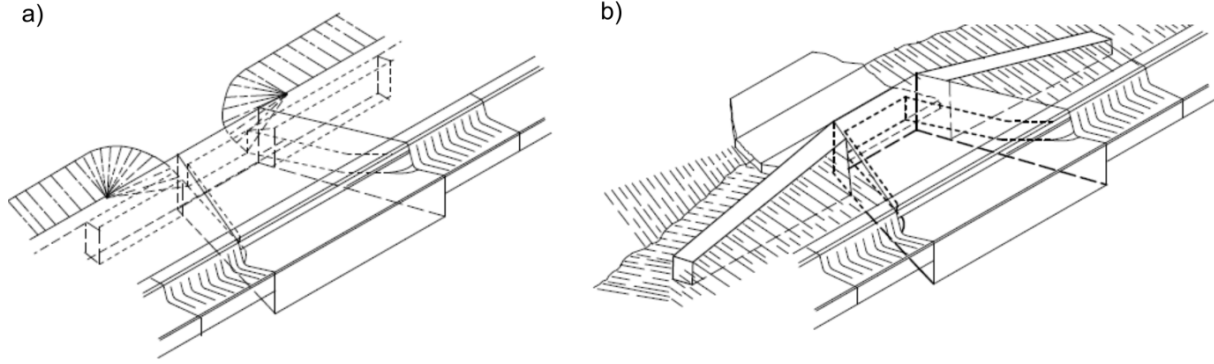


Figure 2: Closed Flume Inlet configurations: a) with sidewalk and b) without sidewalk
(FDOT, 2012)

2.2.2 Flow in Gutters

A pavement gutter is defined as the section of pavement next to the curb which conveys water during a storm runoff event. It may include a portion or all of a travel lane. Gutter cross-sections (Figure 3) can be taken as a triangular shape with the curb forming the near-vertical leg of the triangle. The gutter may have a straight cross slope or a cross-slope composed of two straight planes. Parabolic sections can also be used for the cross-section. Modification of the Manning equation is necessary for computing the flow in triangular channels because the hydraulic radius in the equation does not adequately describe the gutter cross-section, particularly where the top width of the water surface may be much larger than the depth at the curb. To compute gutter flow, the Manning equation is integrated for an increment of width across the section (Johnson and Chang, 1984). The resulting equation in terms of cross slope and spread on the pavement is:

$$Q = \frac{0.56}{n} S^{1/2} S_x^{5/3} T^{8/3} \quad (1)$$

where Q is the discharge (ft^3/s), n is the Manning n value, T is the top width of the flow (ft), S_x is the cross-slope (ft/ft), and S is the longitudinal slope (ft/ft).

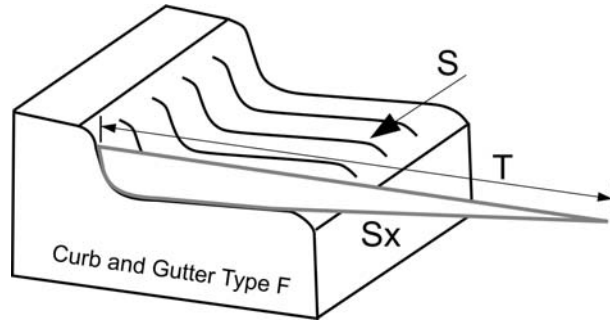


Figure 3: Gutter flow: S and S_x indicate longitudinal slope and cross slopes

2.2.3 Closed Flume Inlet Hydraulic Capacity

The CFI hydrodynamics can be defined similarly to tapered culverts. In essence, the CFI capacity is influenced by water depth at the curb, the opening length, and the height of the curb opening (see Figure-4). CFIs operate as a weir when the depth is lower than the opening height (unsubmerged condition) and as an orifice when the depth is greater than the opening height (submerged condition). Between the two operating conditions, the flow is in a transitional stage.

The equation for the interception capacity of the CFI operating as a weir can be expressed as:

$$Q_i = C_w P d^{1.5} \quad (2)$$

where Q_i is the discharge reaching inlet (ft³/s), C_w is the weir coefficient, P is the perimeter of the inlet (ft), and d is the water depth (ft).

If the CFI operates as an orifice, the orifice equation is applied:

$$Q_i = C_0 A \sqrt{2g(d - C_c h)} \quad (3)$$

where Q_i is the discharge reaching inlet (ft³/s), C_0 is the orifice coefficient, A is the area of opening (ft²), h is the opening of the flume (ft), and d is the water depth (ft). Basically, equations (2) and (3) establish a relationship between the head at the inlet and its discharge. For convenience, we will label this relationship as the CFI performance curve.

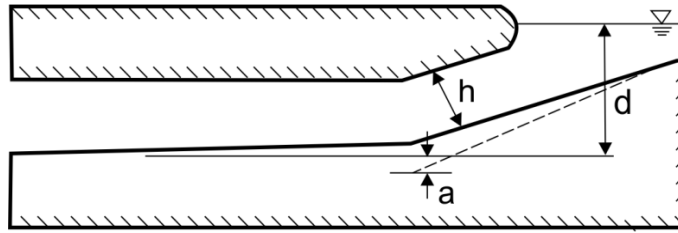


Figure 4: Closed Flume Inlet

A practical procedure to estimate this curve in laboratory conditions is to test the CFI for a range of depths and discharges. The experiments should be conducted with the appropriate density of operating points to obtain reliable support for developing the performance curve. The end result of the experiments is a graph similar to the one illustrated in Figure-5.

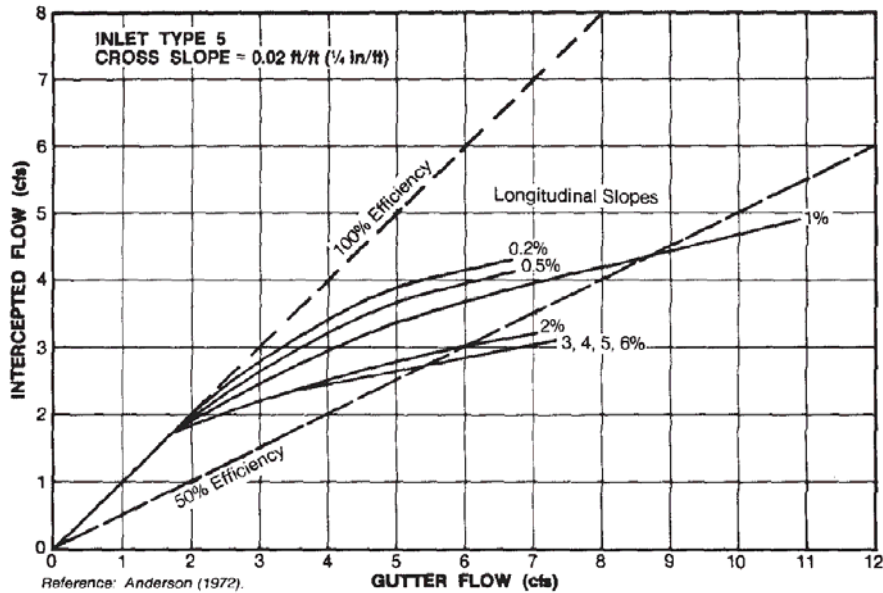


Figure 5: CFI efficiency obtained through hydraulic modeling (FDOT, 2012)

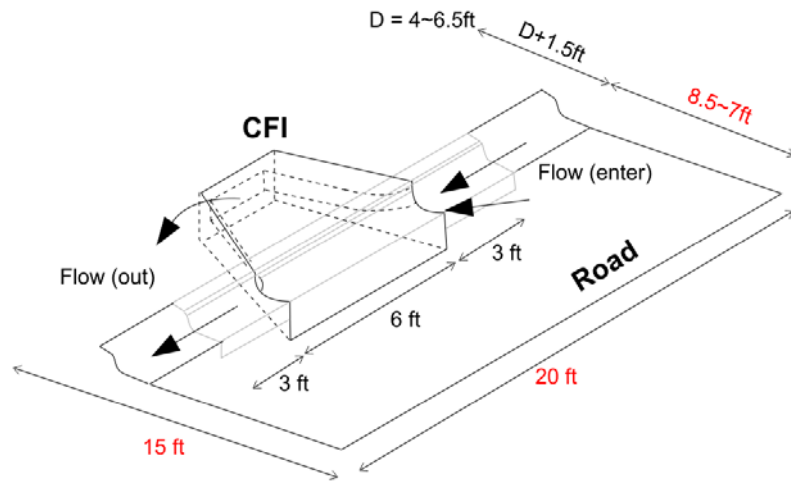
2.2.4 Modifications to the Index 216 FDOT (2014) Geometry

The FDOT RFRP 11/12-021 requested definitive minimum guidelines for the optimization of Closed Flume Inlet hydraulics while handling debris conveyance. For this purpose, the following optimization means (CFI constructive changes) were suggested:

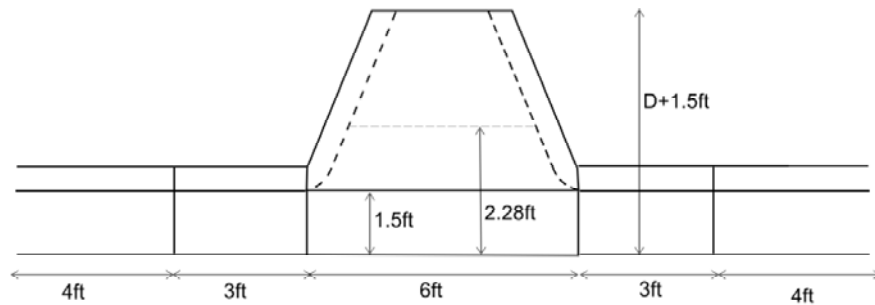
- a) Change of the CFI interior slope;
- b) Change of the CFI interior cross-section
- c) Change in the CFI length

The prototype CFI to be optimized in the study follows the geometry specified in Index 216 of the 2012 FDOT Design Standards as illustrated in Figure-6.

a)



b)



c)

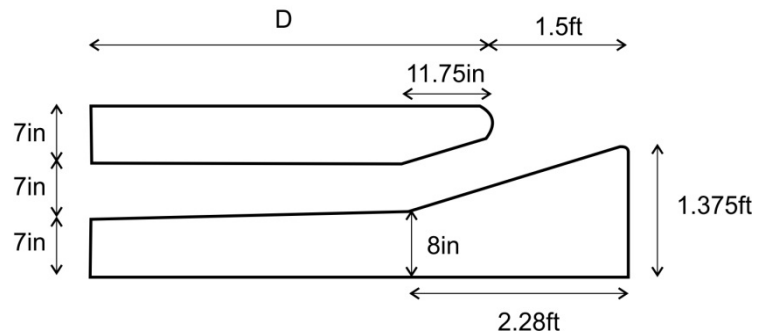


Figure 6: The geometry of the CFI prototype to be investigated in the study:
a) perspective view; b) plan view; c) cross-section view

3. STUDY APPROACH

3.1 Study Objectives

Through documented experiments, this study aimed at finding:

- 1) The optimum CFI interior slope. For this purpose, three CFI interior slopes were investigated. The slopes are defined by setting successively the dimension D in Figure-6 to the following values:
 - a. $D = 4$ ft (without sidewalk)
 - b. $D = 5$ ft (with sidewalk)
 - c. $D = 6.5$ ft (where sidewalk abuts back of curb)

The efficiency of the modified CFIs were assessed based on comparison of the efficiency curves for three longitudinal slopes (0.3%, 2%, and 5%) and three cross-section slopes (0.3%, 3%, 6%) for several gutter discharges in the 1.5 to 12 cfs range . The most efficient slope (optimum) it the one that provides the highest self-cleanup velocity and intercepted flow.

- 2) The optimum CFI interior cross-section. For this purpose the CFI prototype geometry with the (constriction in place) and the constant cross-section configuration (unconstricted) geometry) were investigated. Also tested were CFI configurations with and without the 2-ft extension that were adopted after this project was initiated.

This research objective determined how the change in geometry affects the CFI's self-cleanup velocity and efficiency. The testing protocol was the same as for Objective 1. In accomplishing Objective-2, we used the optimum geometry established through Objective 1.

- 3) The hydraulic capacity of the optimum CFI established through Objectives 1 and 2. The hydraulic capacity determination involved measuring how much of the flow enters the inlet and how much of the flow bypasses the inlet.

The tests for attaining Objectives 2 and 3 are called herein "Screening Tests". The tests for supporting Objective 3 are labeled herein "Performance Tests".

3.2 Phasing of the Investigation Tasks

The phasing of the research is listed below:

TASK-1: Literature Review of Publications Related to Closed Flume Inlets

In executing Task-1, we summarized relevant research, documentation, and reports to support the objectives of the proposed study. Special attention was given to the following topics: the hydraulic capacity of inlets; standards for CFI; the measurement of the hydraulic capacity for inlets; and debris control of the inlets.

TASK-2: Selection of the Optimal CFI Configuration Based on Hydraulic Capacity

In this task, we screened the following CFI configurations:

- Closed Flume Inlet design as specified by FDOT (2014) index 216,
- Constricted vs. unconstricted design (interior cross-section),
- Three different interior slopes on the inlet.

TASK-3: CFI Hydrodynamics and Establishment of the Measurement Protocols

The chief modeling criterion for this study is the Froude number similarity. The relatively large scale of the model (i.e., 1:5) permits accurate modeling of hydraulic performance at the entrance of the CFI. Implications of the Froude modeling similitude criterion on other processes that are developing in the facility were investigated in this task. The measurement procedure and data collection protocols were also established at this point. Finally, the test matrix was elaborated.

TASK-4: Preparation of an Interim Report

After completion of the first three tasks of the proposed study, a summary of the information obtained was presented to FDOT in an interim report. This report led to the final decisions on the physical model design for the CFI reference and modified configurations. The report included the following issues:

- Matrix of modeling experiments (configurations, water flow rates, and sequencing of the experiments);
- Analytical procedures for obtaining the performance curves
- Format of the resulting presentation and;
- An analysis of the gap between the current and desired state of practice with respect to addressing issues in CFI operations.

TASK-5: Construction, Calibration and Debugging of the CFI Physical Models

After completion of the model construction, the experimental instruments were installed. Calibration and verification of several instruments was also carried out. A series of tests were conducted to check the model operation, repeatability and stability of the flow conditions.

TASK-6: Tests for Selection of the Optimum CFI (Screening Tests)

The objectives of this task were to sample the CFI performance curves for establishing the optimum modification to the prototype CFI. The set of tests included the reference CFI (as-is geometry) and the modified CFI configurations proposed by FDOT: interior slope, constricted vs. unconstricted, extended vs. non-extended.

The following data was collected for each of the tests:

- Water level at the entrance of the inlet;
- Flow rate approaching the inlet; and
- Flow rate intercepted by the CFI

During these tests the research team was in constant communication with FDOT. Individual test results were shared with FDOT for decision making of the next modeling step.

TASK-7: Tests for Establishing Efficiency CFI Curves (Performance Tests)

The optimum geometry established through the investigations conducted in Task-6 was tested over a range of hydraulic conditions. The hydraulic efficiency was captured through analysis into graphs. During these tests, the following data was collected:

- Water level at the entrance of the inlet;
- Flow rate approaching the inlet; and
- Flow rate intercepted by the CFI
- Self-cleaning velocity in the CFI

The density of measurements for the Performance Tests was higher than for the Screening Tests to obtain smooth curves readily usable for design purposes.

TASK-8: Final Report Preparation

The Final Report of the research project is prepared to demonstrate the investigation findings. It includes all aspects of the investigation and multi-facet presentation of the

results. We produced several video recordings and static photos of the facility during the tests to enhance the presentation of project outcomes.

3.3 Modeling Matrix

3.3.1 Screening Tests

In Task 2 of the study, a phased approach was used to gradually test various geometries for the CFI design to determine the optimum configuration with respect to hydraulic operation (Table-1). Prior to the screening tests, a series of flows with the original CFI geometry were tested to verify the flow conditions throughout the hydraulic model and the repeatability of the tests results for one setting. These preliminary results indicated a good repeatability and stability of the model operation and the adequacy of the instrumentation for documenting the global flows through the model. Subsequently, each CFI geometry was tested for a range of longitudinal slopes in order to verify the hydraulic performance on a significant range of the possible flows through the structure.

Table 1: Modeling scenarios for the screening tests

Maximum modeled flow: 12 cfs (according to the specifications Storm Drain Handbook flowcharts) CFI operation: inlet control (the downstream CFI exit is releasing with free fall)		
CFI constructive changes		
1. Interior slope	2. Interior cross-section	3. Inlet with/without sidewalk inlet
<p>3 slopes</p> <p>H = 7" is constant for all cases. D = 4 ft (without sidewalk) D = 5 ft (with sidewalk) D = 6.5 ft (where sidewalk abuts back of curb).</p>	<p>2 cross-sections</p> <p>for optimum geometry obtained in step 1</p> <p>constricted</p> <p>Unconstricted</p>	<p>4 Length for the unconstricted structure</p> <p>4-ft unconstricted without sidewalk inlet</p> <p>4-ft unconstricted with sidewalk inlet</p>

3.3.2 Performance Tests

The following tests were conducted with the model set for the CFI optimal configuration established through the screening tests. This test series is labeled in this report “Performance Tests.” A much more dense series of slopes for the cross-section and longitudinal positioning was used. The matrix of slopes for the Performance Tests, is provided in Table-2. As for the Screening tests the gutter discharge varied from 1.5 to 12 cfs (prototype units) in fine increments. In addition to the typical measurements taken in the Screening Test series, the Performance Tests included estimation of the mean velocity across the CFI cross-section to compare its prototype values with the self-cleaning velocity (2 ft·s). For the flow range tested in this study, the CFIs have not attained total submergence, flow situation where the inlets act as orifices rather than free-surface flow structures.

Table 2: The longitudinal and cross-section slopes used for the Performance Tests

Longitudinal Slope			Cross-Slope		
No.	% Slope	Angle (deg)	No.	% Slope	Angle (deg)
1	0.3	0.17	1	2	1.15
2	1	0.57	2	3	1.72
3	1.5	0.86	3	4	2.29
4	3	1.72	4	5	2.86
5	4	2.29	5	6	3.43
6	5	2.86	--	--	--

4. EXPERIMENTAL FACILITIES AND PROCEDURES

4.1 Scale Selection and Similitude Criteria

Accurate simulation of flows in a laboratory model requires geometric, kinematic, and dynamic similarity. However, it is not possible to achieve similarity of all forces, so similarity is sought only among the dominant forces. So-called model-scale effects are caused by the absence of similitude between the minor forces, and should be minimized if possible. Flows that involve free surfaces, such as in the modeled roadway and CFI, are dominated by gravitational, inertial, and pressure forces. The Froude number is the ratio of inertial to gravitational forces and represents the dominant parameter in free-surface flows. Kinematic similarity requires that the Froude number be the same in model and prototype.

IIHR chose an undistorted Froude length scale of 5. This scale permits accurate modeling of inlet head box and weir, roadway and CFI. Froude scaling relationships were applied to calculate expressions relating model and prototype values. These expressions are summarized in Table-3.

Table 3: Model similitude criteria based on a 1:5 length ratio

Variable	Relationship Prototype/Model	Model Scaling Factor
Length	$L_r = L_p/L_m$	5
Area	$A_r = L_r^2$	10
Volume	$V_r = L_r^3$	125
Slope	$S_r = L_r/L_r$	1
Velocity	$V_r = L_r^{0.5}$	2.236
Time	$t_r = L_r^{0.5}$	2.236
Discharge	$Q_r = V_r * A_r = L_r^{2.5}$	55.902
Pressure	$\rho_r = L_r$	5
Force	$F_r = L_r^3$ (same densities)	125
Reynolds Number	$Re_r = L_r^{1.5}$	11.180

4.2 Test Facilities

The model was constructed in IIHR's Model Annex located near downtown Iowa City. The 14,000-ft² Hydraulics Model Annex (HMA) provided ample research space within close proximity to research staff. HMA and adjacent buildings house IIHR's Mechanical Shop staff which provided support for model construction and modifications throughout the project.

4.3 Model Construction

The CFI model was constructed of materials with dimensionally stable properties when exposed to water. Steel and plastic pipe conveyed water from the pump to the inlet pipes. Brass gate valves controlled inlet flows to the model headbox. The model's headbox, roadway surface, and outlet weir box were constructed from marine grade plywood. Computer numerically controlled (CNC) milled high-density polyethylene (HDPE) ribs provided supports underneath the roadway which could be shimmed to set the desired cross-slope. The model gutter was formed with a series of CNC-milled polyvinyl chloride (PVC) templates that were filled with concrete. A screed was used to form the final curb surface which was subsequently painted with two-part epoxy paint. The various CFI attachments were built from CNC milled translucent Plexiglas and incorporated a bolted flange that could be easily removed and replaced at any time. Structural steel frame members provided ample support along the model test section to avoid deflections in the roadway and curb surfaces. Sets of removable vertical support legs and a pillow block bearing at the downstream end provided adjustability to the longitudinal slope of the model. Engineering drawings of the CFI model are provided in Figure-7 and Figure-8. 3D renderings of the model are shown in Figure 9 and Figure 10. Figures 11 and 12 show photographs of the completed model.

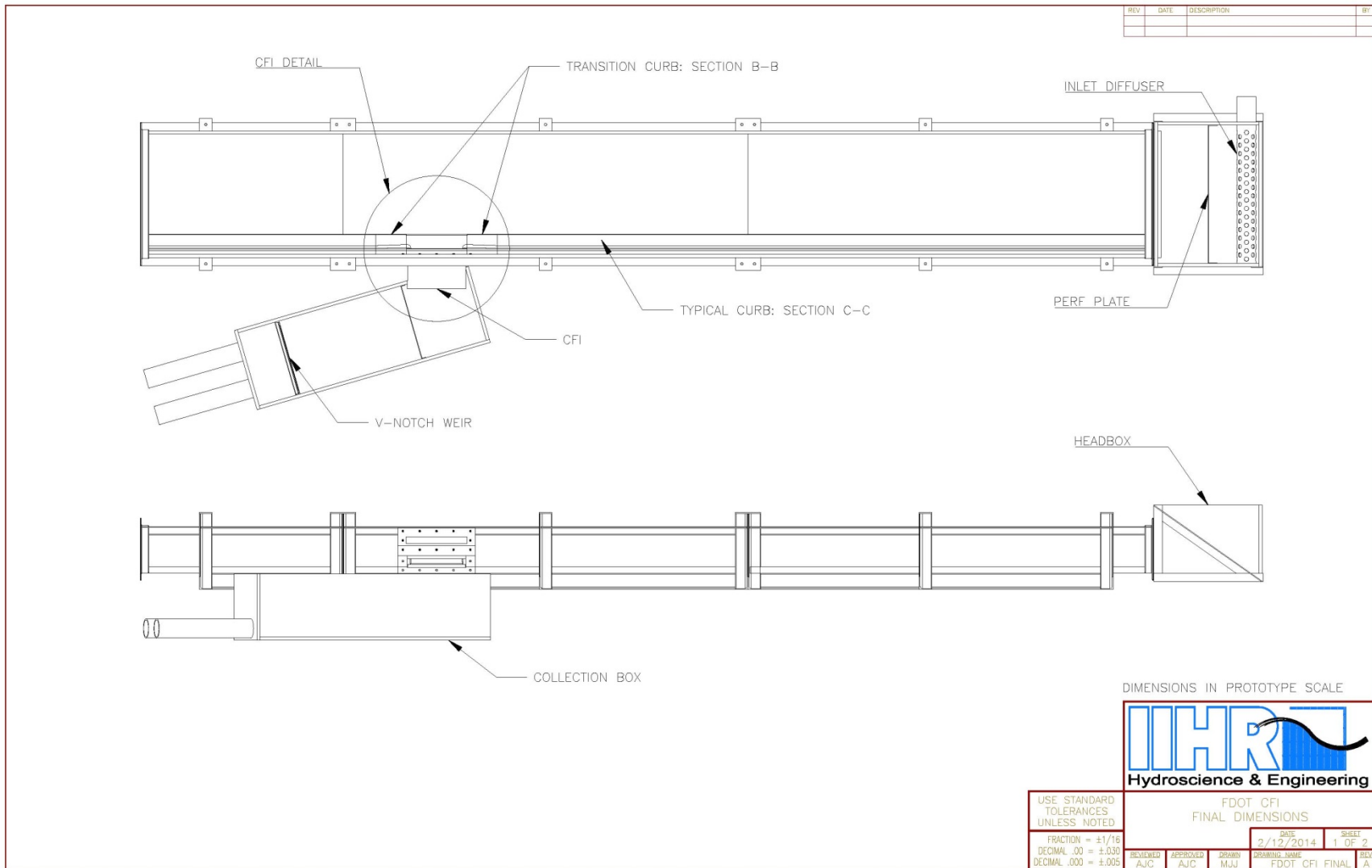


Figure 7: Plan and Elevation views of CFI model

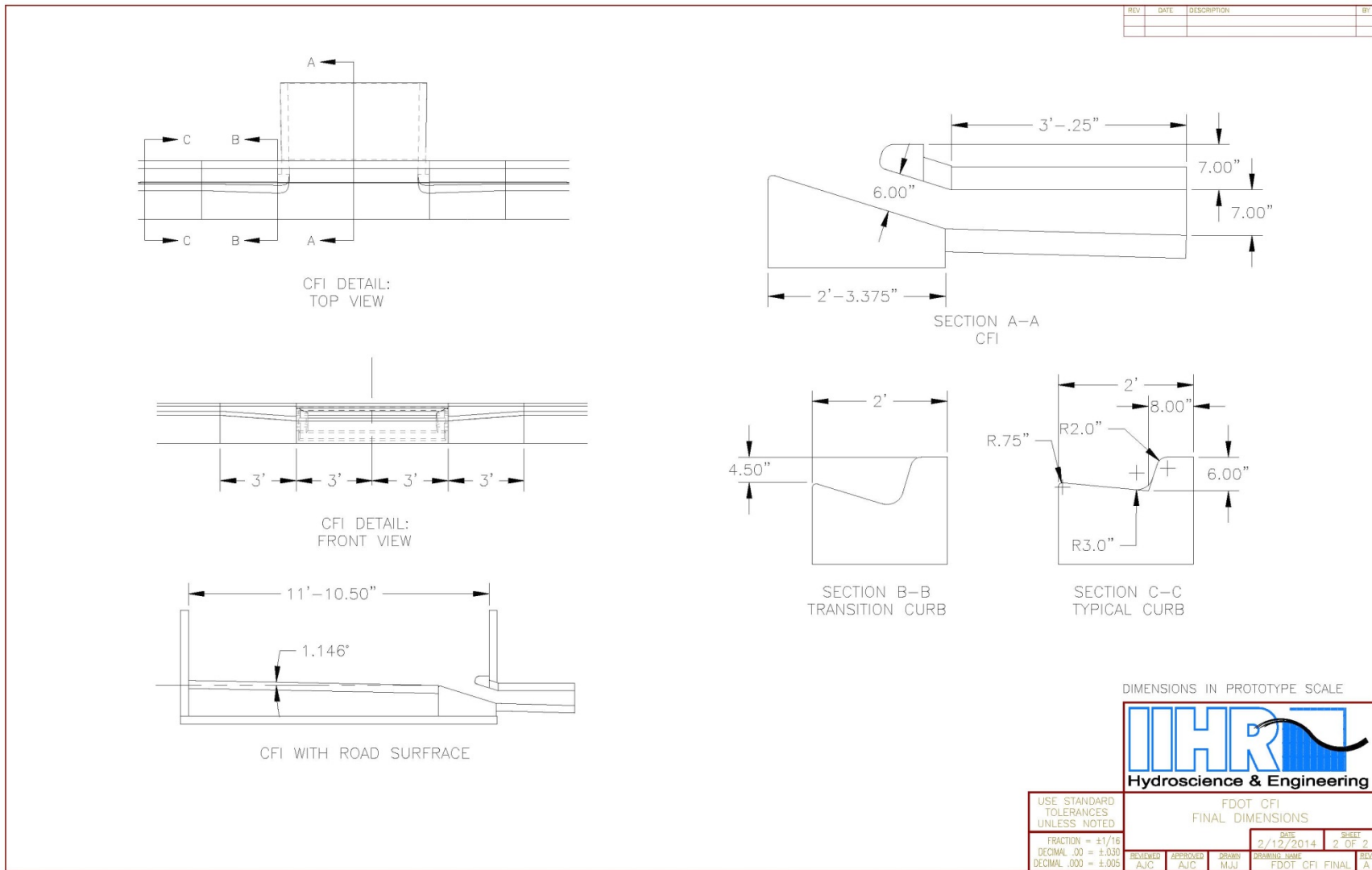
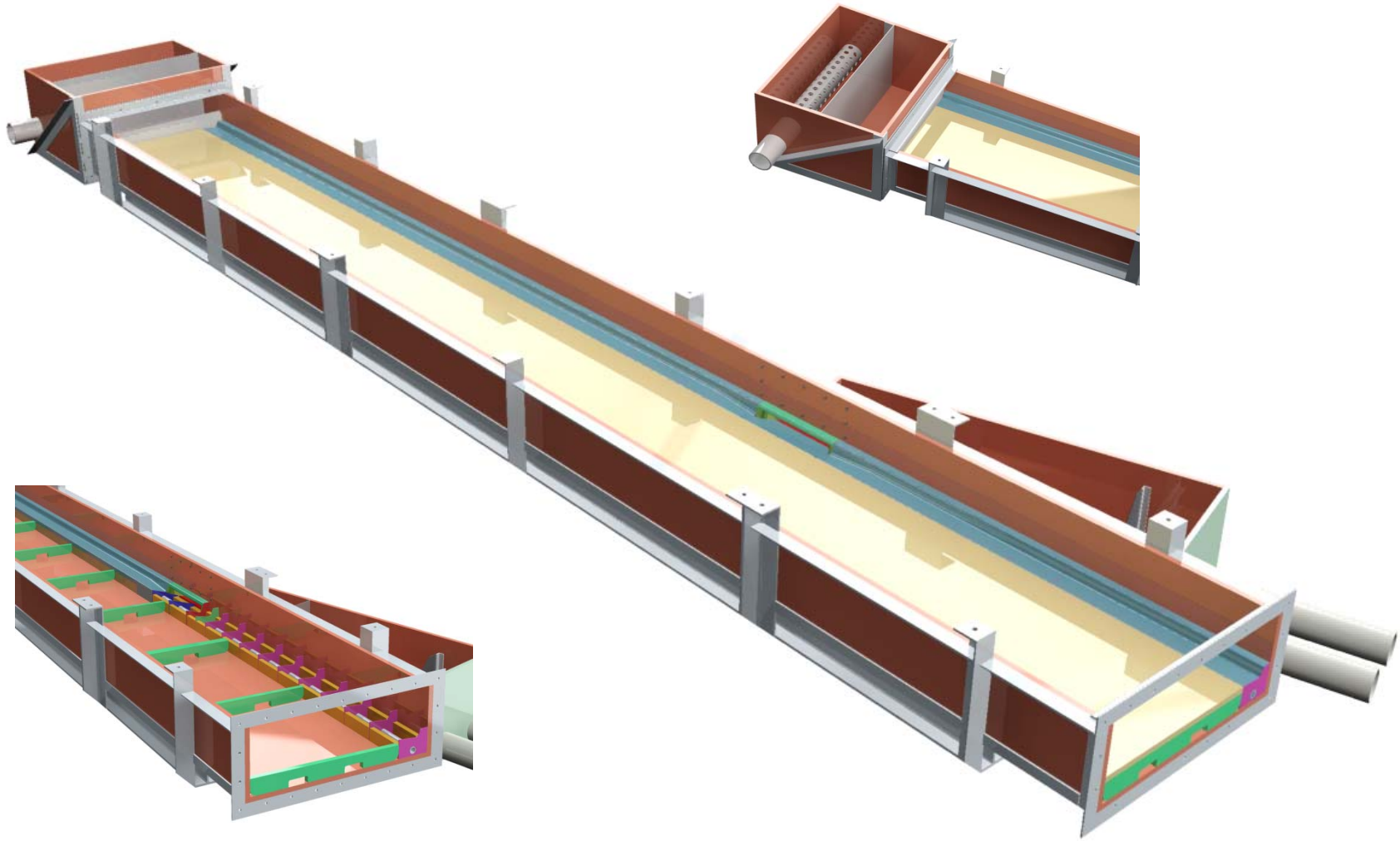


Figure 8: Model detail and section views (2% cross slope shown)



**Figure 9: Upstream perspective view of CFI model
(including close-up views of the headbox and of the internal structure of the roadway and curb)**

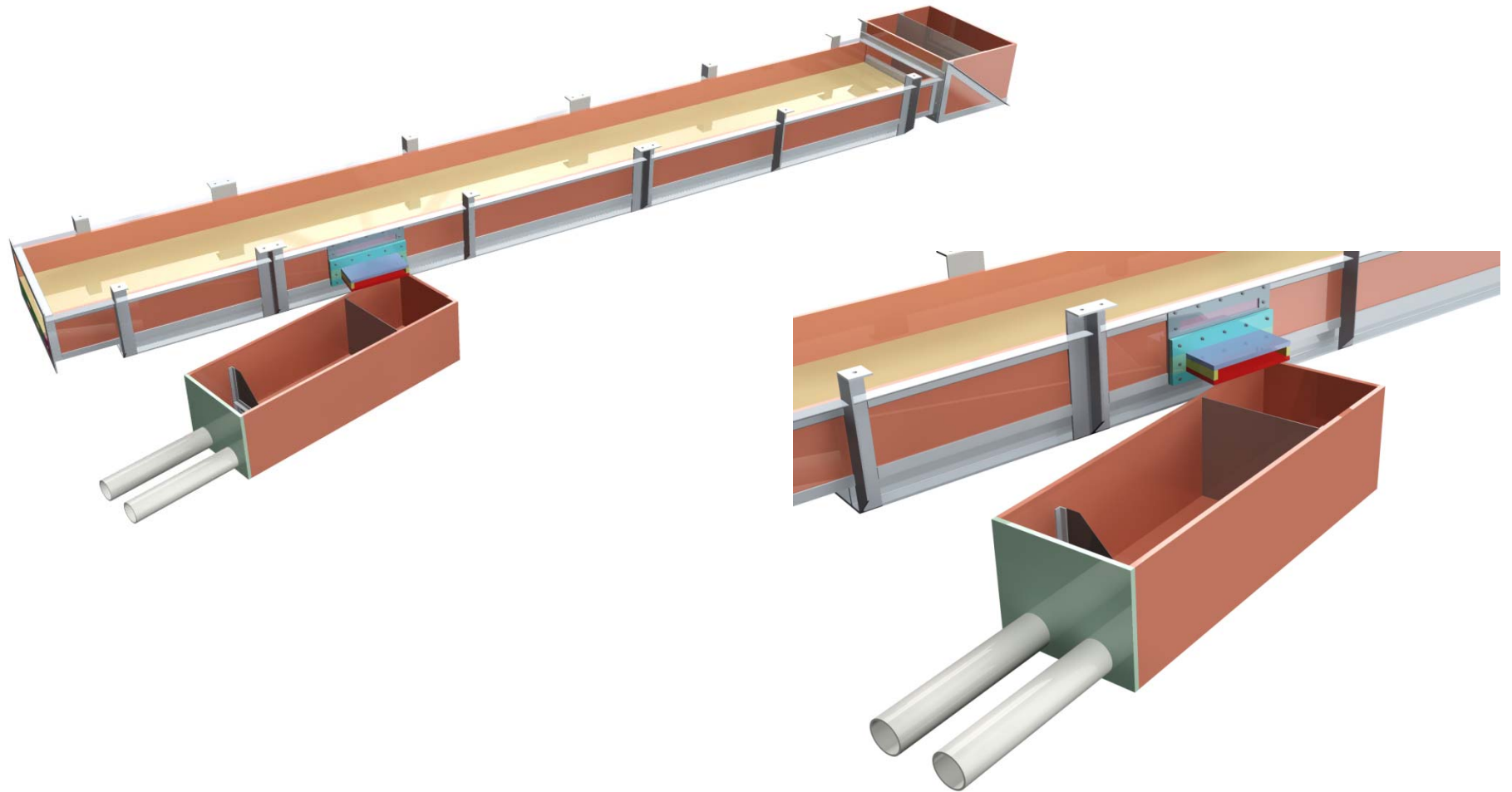


Figure 10: Upstream view of v-notch weir box and model including a close-up of the weir box

a)



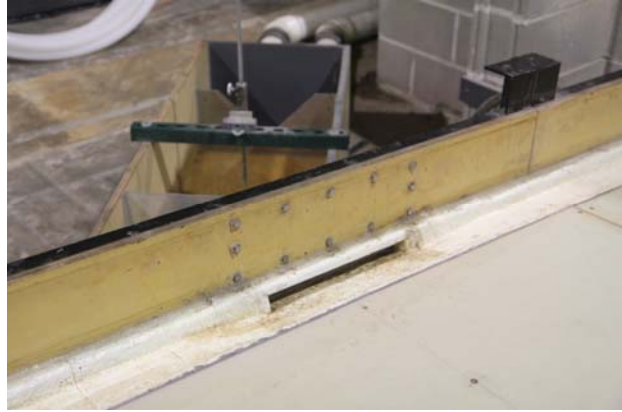
b)



Figure 11: Rendered photo of the model a) seen from downstream, b) seen from a side



a)



b)



c)



d)



e)



f)

Figure 12: Photographs of the various parts of the model (final CFI installed)

4.4 Flow Conveyance and Measurement

A 75 hp pump with variable frequency drive (VFD) controller supplied water to the model. Water was pumped through a 12-inch PVC pipe main from the sump under the laboratory floor and then through sections of either 1/2-inch (low flow) or 2-inch (high flow). Control of model

flow rates was provided by gate valves in the feed lines and the VFD. Inflows to the model were measured with GPI turbine meters (model TM075-N (low flow) and model TM200-N (high flow)) with stated accuracies of +/- 3% of reading. The flow meters were installed to ANSI standards. Intercepted CFI discharges were measured with a v-notch weir situated in the collection box (Figure-7, Figure-12). The flow exited through the CFI and was conveyed to the collection box which was equipped with flow conditioning and a v-notch weir that facilitated direct measurement of the intercepted CFI discharge. The head on the weir was measured with a point gage with vernier scale accurate to +/- 0.0005 feet. Discharge was then calculated with equation 4.

$$Q_{v\text{-notch}} = 2.5 \times H^{2.5} \quad (4)$$

Where $Q_{v\text{-notch}}$ is the intercepted CFI discharge in cubic feet per second (cfs) and H is the measured head above the v-notch weir in feet. The v-notch weir was fabricated and installed according to The United States Bureau of Reclamation Water Measurements Manual. A comparison was made between the inflow turbine meters output and the theoretical v-notch weir equation (equation 4) to ensure accuracy and an acceptable agreement between the two. The comparison is provided in Figure-13.

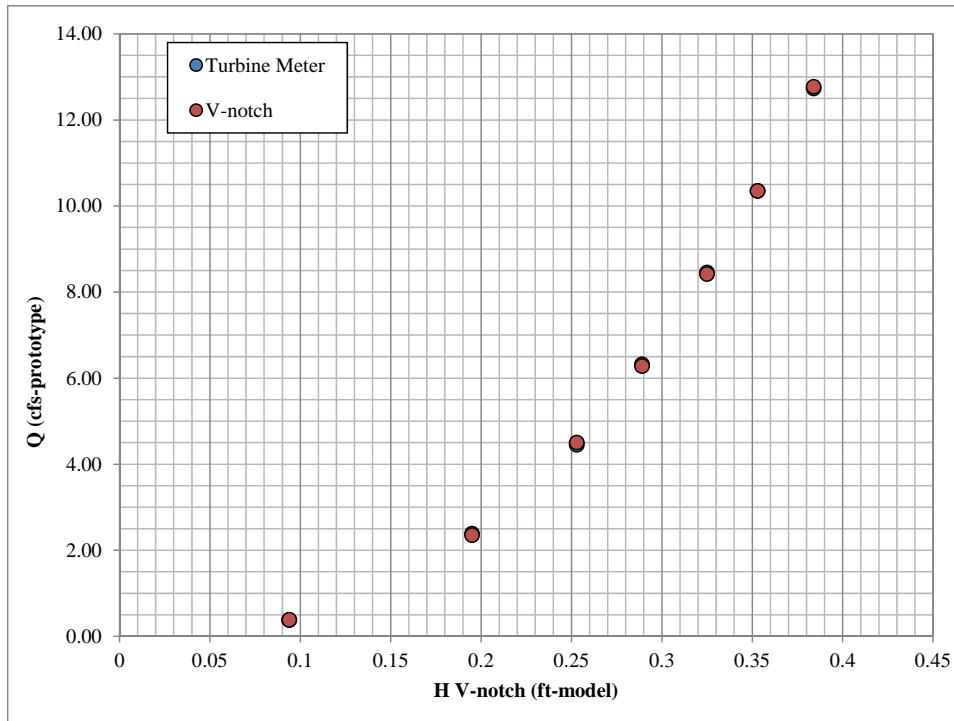


Figure 13: Comparison of output from turbine meter and v-notch weir equation over the full range of flows to be tested

4.5 Measurement Protocols

For each set of measurements, care was taken to be sure the model cross-slope and longitudinal slopes were set correctly and consistently. Pre-fabricated sets of spacers were installed to set the proper longitudinal slope, and shims were added to fine-tune the settings. A 6-foot-long level and digital protractor were used to ensure that the longitudinal slope was consistently accurate to within 0.05 degree (0.09% slope). Similarly, the cross-slope was set by inserting shim spacers to the uphill side of the roadway supports, and a 2-foot level and digital protractor were used to check the cross-slope at each support.

Individual CFI attachments were inspected to ensure the proper angle between the floor and ceiling, and once installed, the ceiling was set to level. Model inflows were established and allowed to stabilize for 5 minutes prior to measurement of the CFI discharge.

The measurement of the cross-section velocity was done with an innovative method. Specifically, for each tested flow for the performance curve, a photo of the flow leaving the CFI was taken from above the V-notch weir box (see Figure-12.f). Such a photo is presented for illustration purposes in Figure 14. Using these photos, image analysis and direct measurements of the water depths at several locations at the CFI outlet cross-section, the area of the cross-section occupied by fluid was estimated for each flow situation. Knowing the flow intercepted by CFI and the cross-section area estimated above, the average cross-section velocity can be obtained.



Figure 14: Photos of the downstream CFI cross-section used to determine the average-cross-section velocity

5. EXPERIMENTAL RESULTS

5.1 Screening Test Results

The screening tests entailed testing of 5 different CFI geometries as illustrated in Table-1. The first set of the screening tests was focused on evaluating the effect of the CFI interior slope. For this purpose tests with the 6.5-ft, 5.0-ft, and 4.0-ft long inlets were run (see Table 1, column 1). Following the assessment of this initial series of screening tests, decision was made in consultation with FDOT that the 4-ft CFI was performing better. Consequently this geometry was selected for further screening tests with changes applied to other geometrical characteristics of the 4-ft long CFI. This second series of tests were focused on comparing the effect of constriction on the CFI performance using the 4-ft long CFI selected in the first series of tests as a starting point (see Table-1, column 2). The results indicate that the unconstricted CFI is performing better than the constricted one. During the conduct of the study, an additional geometry was added to the original screening tests at the request of the client. Specifically, a 07/01/2013 revision was brought to the CFI cf. Index 216 (FDOT, 2014). The revision recommends the addition of a sloped section to the outlet when the CFI is associated with a sidewalk (see Appendix B). The CFI geometry with the 2-ft down-sloping extension is sketched in see Table-1, column 3. Figures 15 to 19 provide renderings of all CFI configurations tested during the screening tests. The results of the tests conducted in the screening phase are illustrated in Figures 20, 21 and 22.

Figure-20 illustrates the effect of the interior slope change. The tests, conducted with several longitudinal slopes (i.e., 1.5%, 3%, and 5%), illustrate that there is practical no difference in the hydraulic efficiency of the 6.5-ft-long and 4-ft-long configuration CFIs for any of the longitudinal slopes. The 5.0-ft-long CFI displayed a slightly better performance for all the tested longitudinal slopes. However, given that the CFI performance improvement was present mostly for the larger flows (i.e., larger than 4 cfs) and as most of the storms are in the range of 0 to 4 cfs, the research team and the FDOT project manager jointly decided to select the 4-ft-long CFI as the qualified CFI candidate. Moreover, the 4-ft-long CFI is currently in production and the change in specifications will require the industry to change the production lines accordingly.

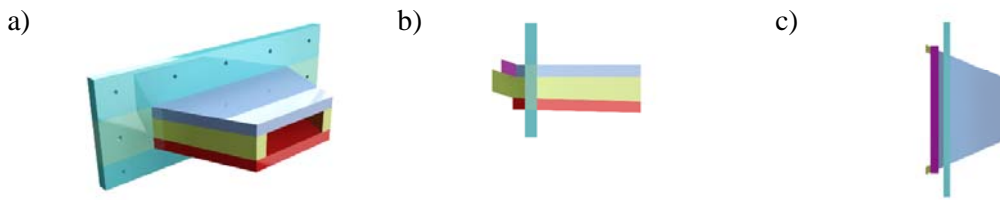


Figure 15: Constricted CFI model with D = 4ft: a) perspective view, b) side view, and c) top view

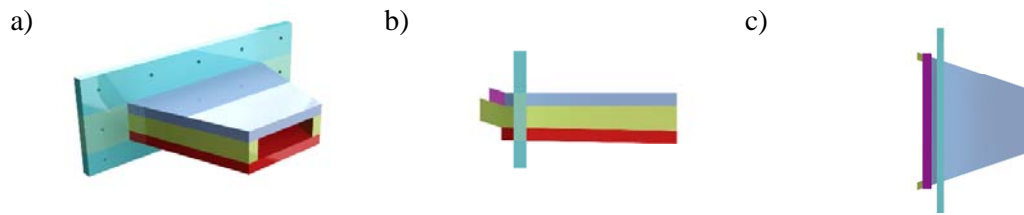


Figure 16: Constricted CFI model with D = 5ft: a) perspective view, b) side view, and c) top view

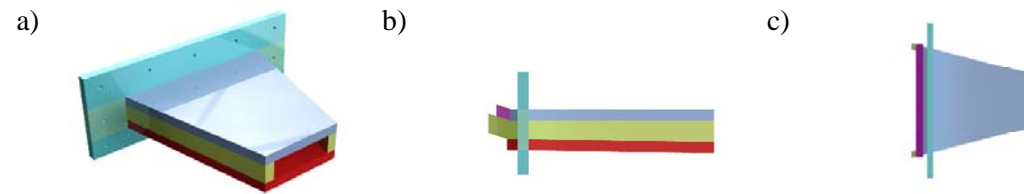


Figure 17: Constricted CFI model with D = 6ft: a) perspective view, b) side view, and c) top view

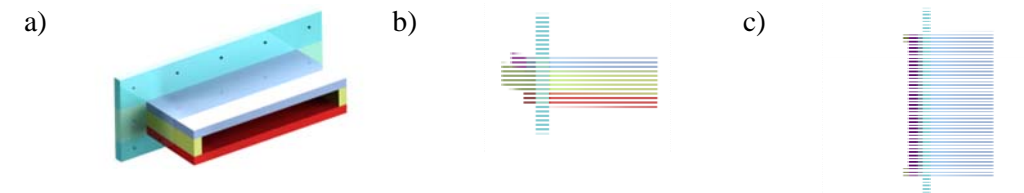


Figure 18: UnConstricted CFI model with D = 4ft: a) perspective view, b) side view, and c) top view

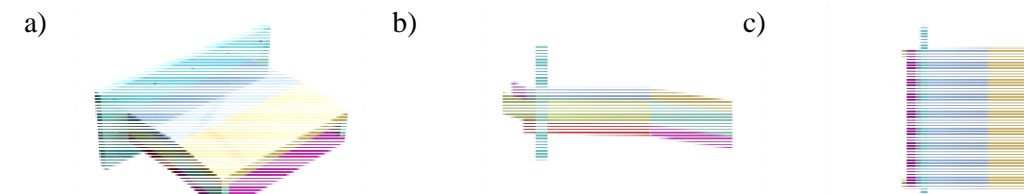
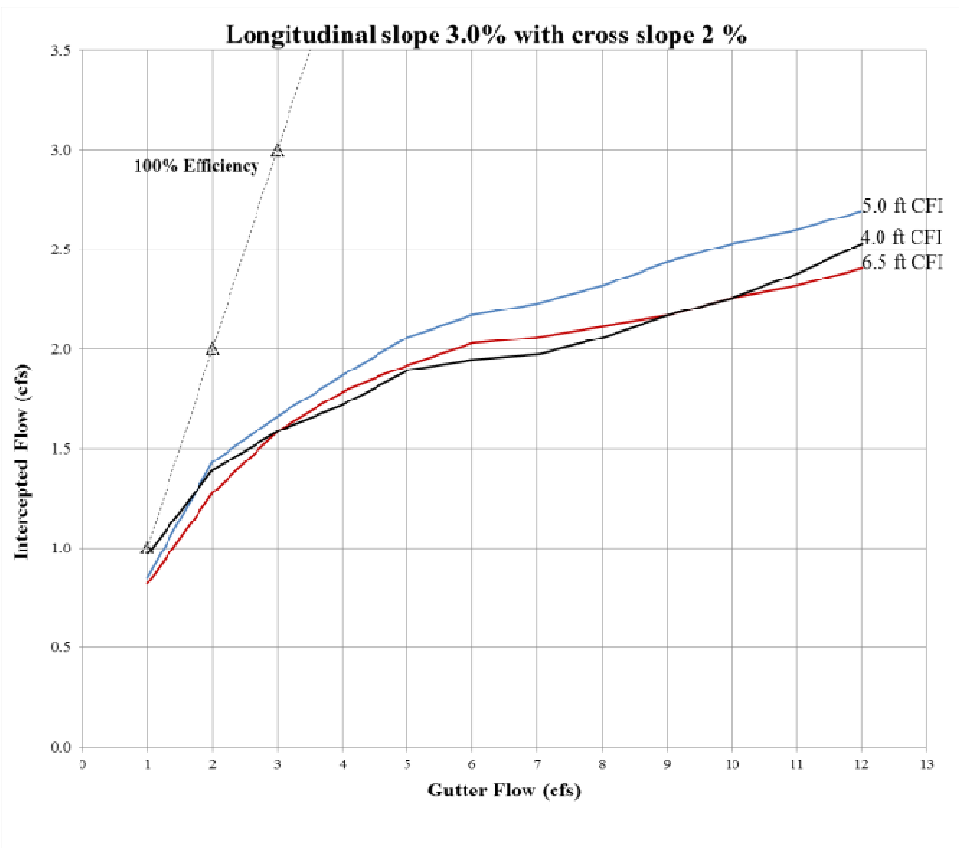
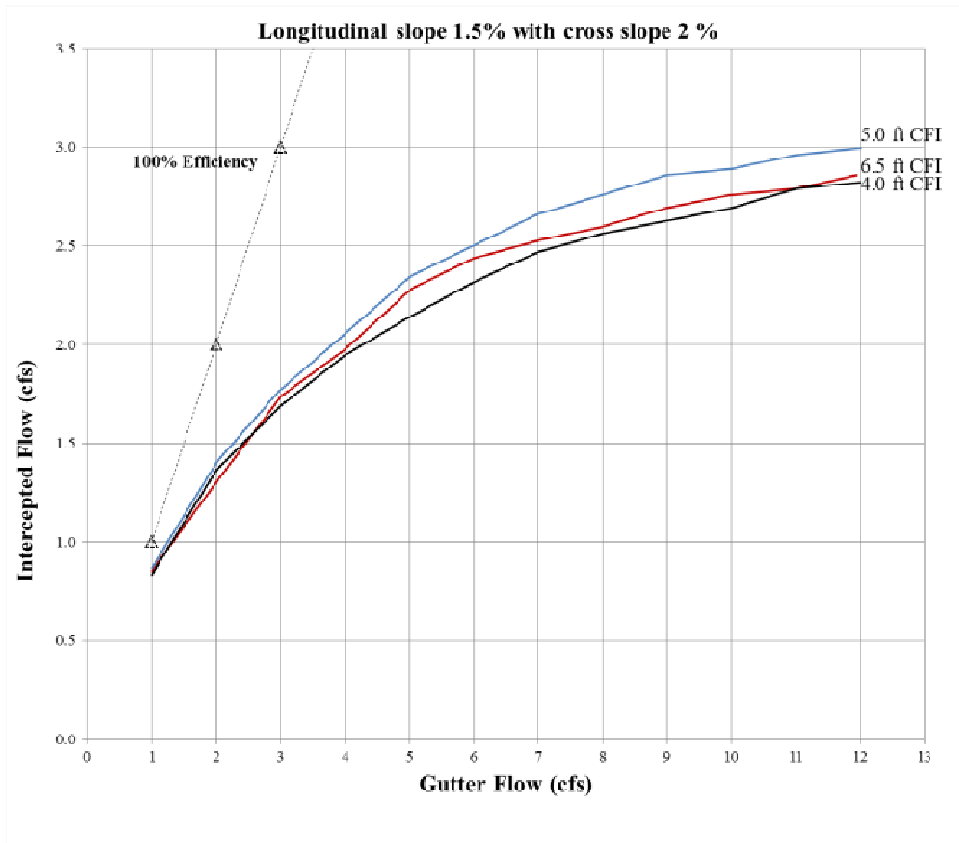


Figure 19: Side view of the unconstricted CFI model with D = 4ft and sidewalk inlet

Source: FDOT 2014 Design Standards, Index No. 216, (07/1.13)



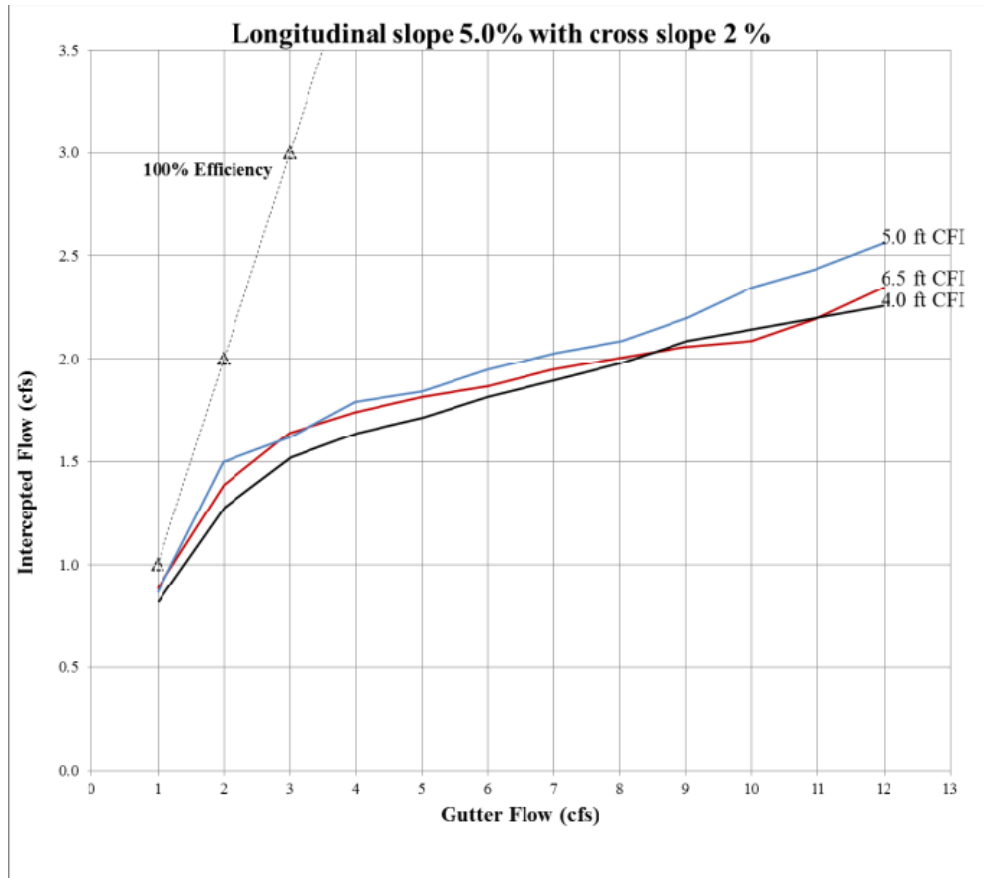


Figure 20: The effect of the CFI interior slope screening tests.

The tests include the 6.5-ft-long, 5-ft-long, and 4-ft-long CFI. Due to the configuration constraints, a change in the interior slope of the CFI leads to a change in the length of the CFI.

The next series of screening tests compared the 4-ft-long constricted and unconstricted CFI configurations. The results of these tests are displayed in Figure-21. These tests were conducted over the same range of longitudinal slopes as in the first series of screening tests, i.e., 1.5%, 3% and 5%. As illustrated by the plots in Figure-21, there is practical no relevant distinction between the 4-ft-long unconstricted and the 5-ft-long CFI. As a reminder, we will note that the 5-ft-long CFI geometry was not selected as a viable candidate in the first series of screening tests as the slight enhanced performance compared with the 4-ft-long constricted CFI does not warrant the change in the production line of the CFI construction. However, the superior hydraulic performance of the unconstricted 4-ft-long CFI compared to 4-ft-long CFI for all flow ranges and longitudinal slopes determined the study team (in consultation with FDOT) to select as candidate for optimum geometry the 4-ft-long unconstricted CFI. It should be mentioned that the

constricted CFI does not require extensive changes in the manufacturer production process. The unconstricted configurations were proposed by CFI manufacturers for efficiency in production, i.e., to enable the constructor/precaster to remove the casting forms through the back of the inlet.

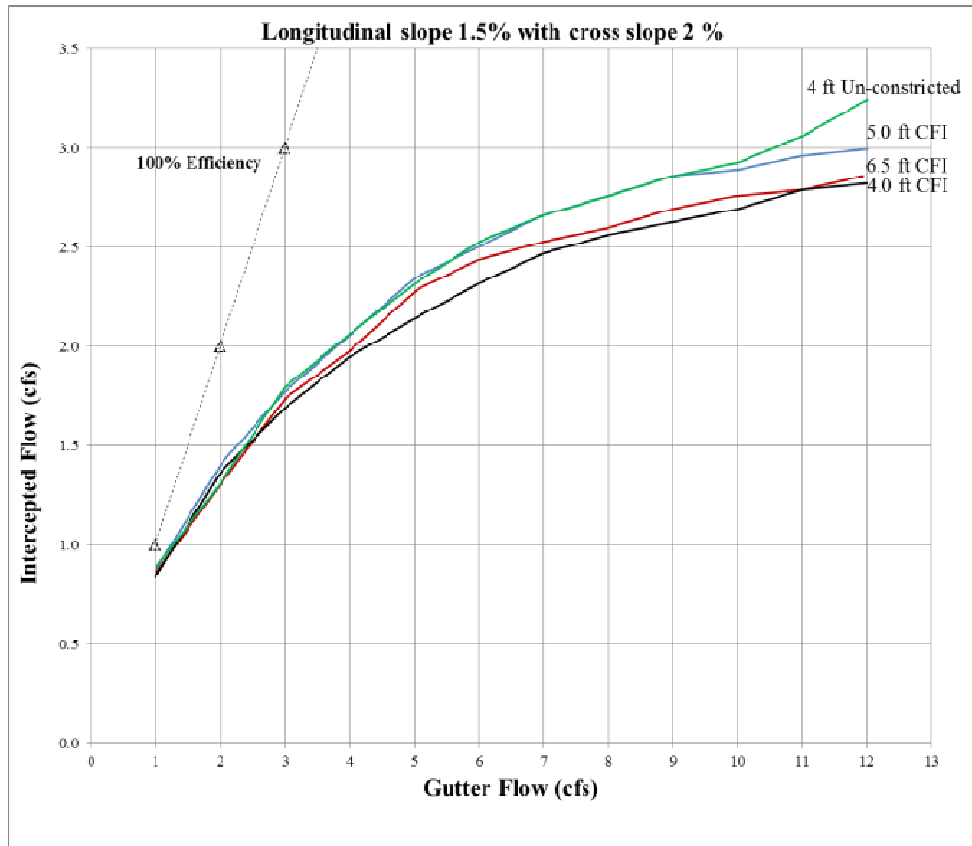


Figure 21 (Part 1): The effect of the CFI constriction screening tests

(continued on next page)

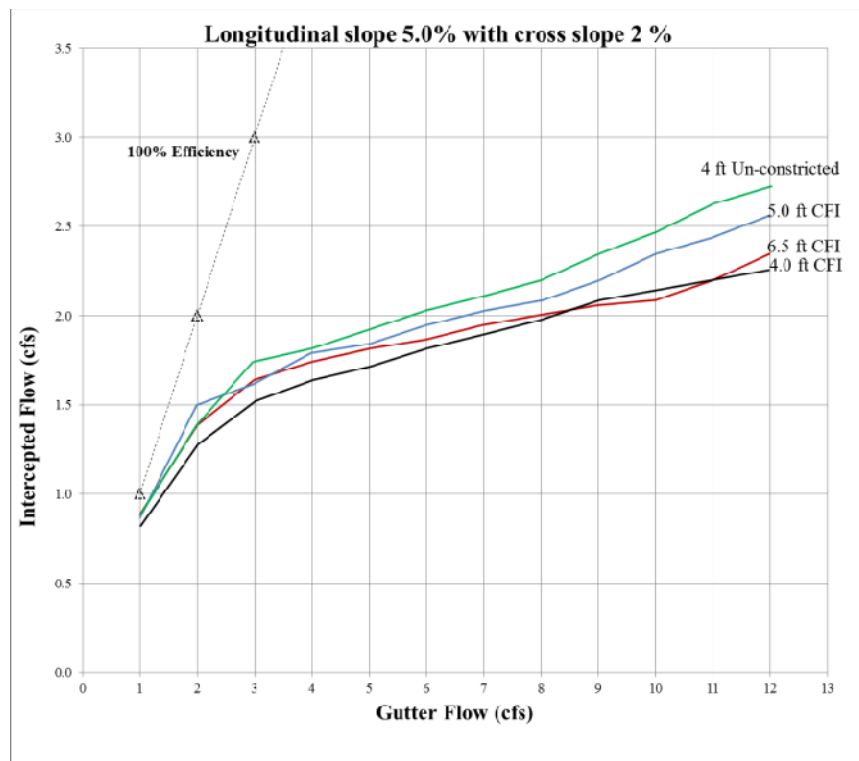
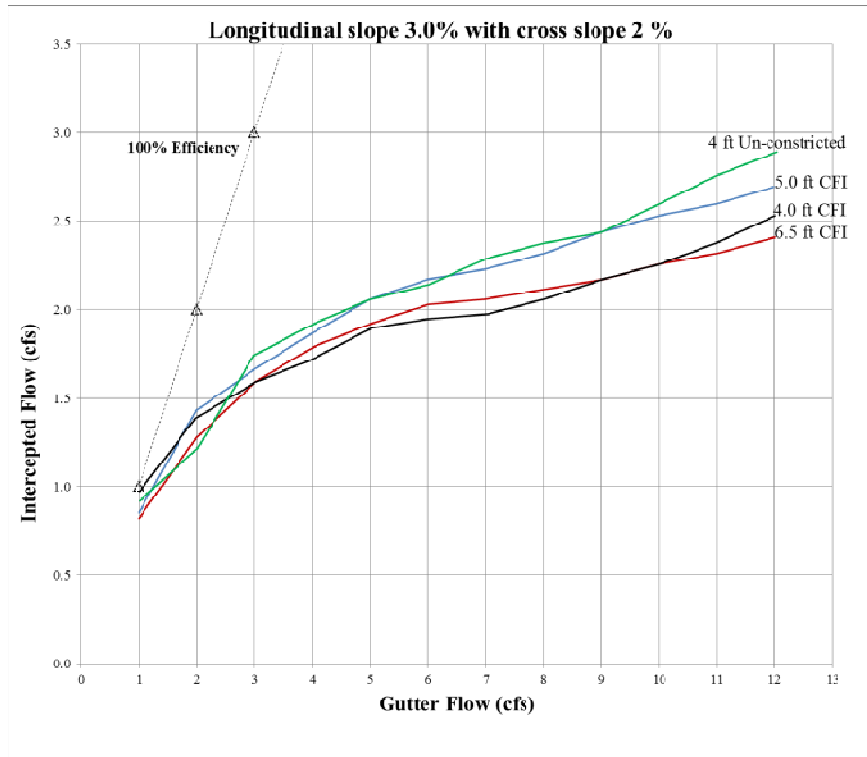


Figure 21(Part 2): The effect of the CFI constriction screening tests
The tests include the original 6.5-ft-long, 5-ft-long, and 4-ft- long CFI and the unconstricted 4-ft-long CFI.

During the conduct of the study, a new type of CFI started to be implemented on various Florida DOT roads: a sloping 2-ft-long extension, which is added to current CFIs. The addition is mostly motivated by aesthetical reasons. The configuration of the modified inlet is provided in Figure 19. Tests were performed to determine if the addition to the culvert changed the CFI efficiency in any way. The results of these additional tests are provided in Figure 22. The results clearly illustrate that there is no difference in the hydraulic performance of the 4-ft-long unconstricted CFI with and without extension.

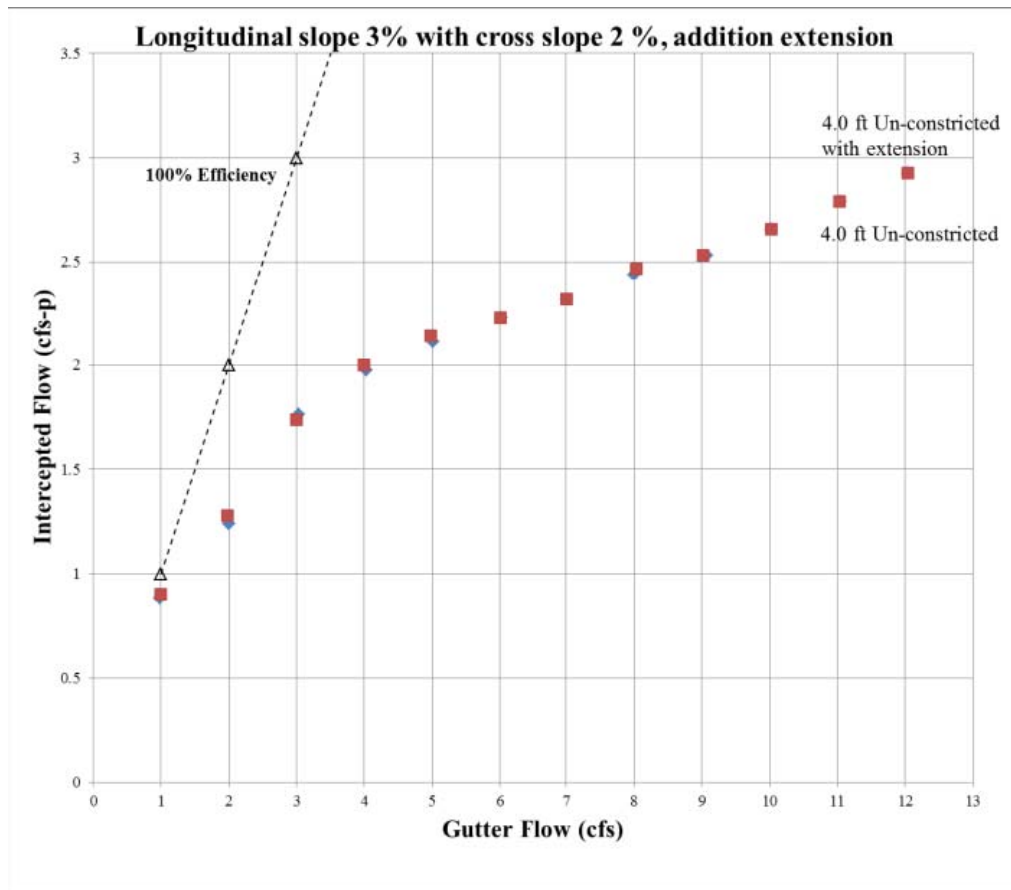


Figure 22 (Part 1): Screening tests for evaluating the effect of the addition of the 2-ft-long sloping CFI extension (see Figure 5)

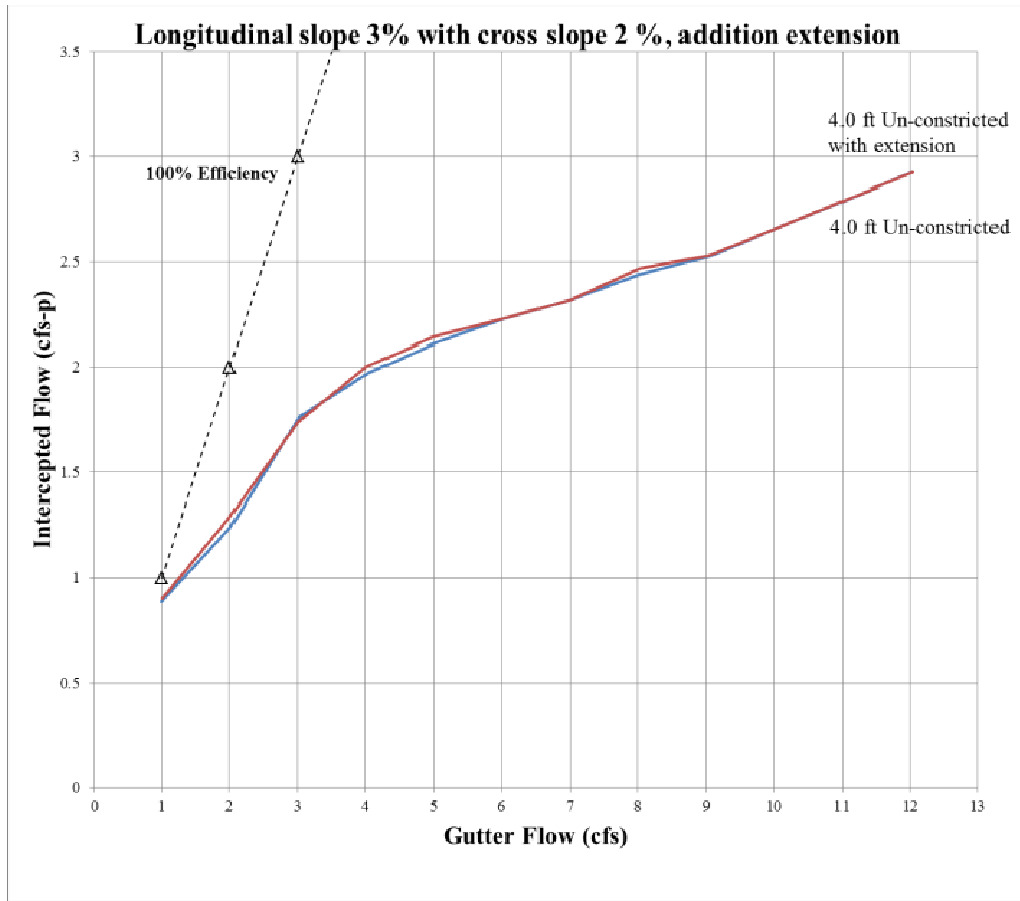


Figure 22 (Part 2): Screening tests for evaluating the effect of the addition of the 2-ft-long sloping CFI extension (see Figure 5)

In summary, the screening tests aimed at evaluating the CFI optimal configuration entailed assessment of the hydraulic performance of:

- a) three interior CFI slopes
- b) constricted vs unconstricted CFI barrel
- c) CFI with and without 2-ft-long sloping extension at the barrel outlet

The results of the hydraulic tests using these CFI geometries lead the investigation team under the supervision of the project manager to the conclusion that the 4-ft-long unconstricted CFI is the optimal candidate for implementation.

5.2 Performance Test Results

5.2.1 Performance Curves

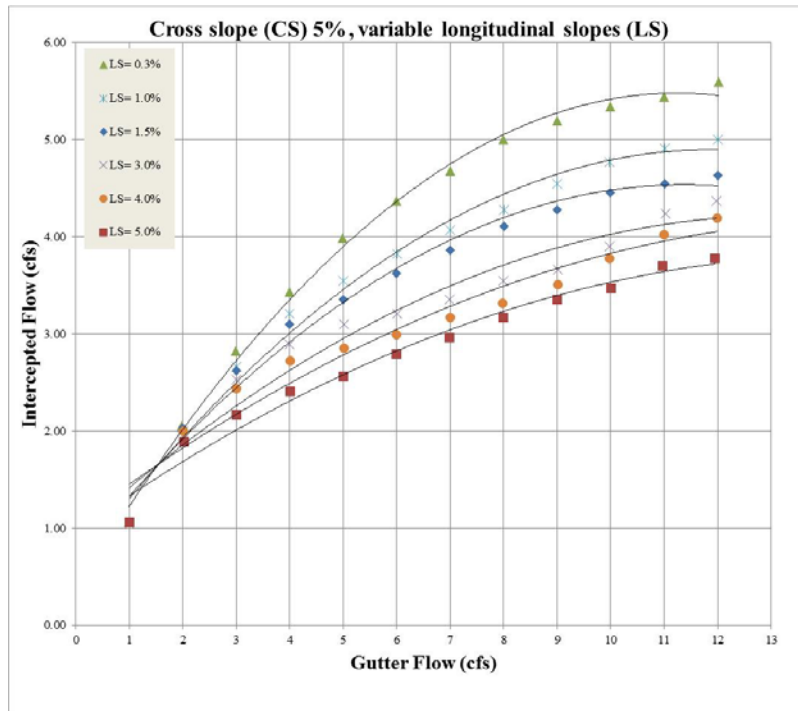
The remainder of the study will focus on testing the identified optimal CFI candidate: the 4-ft unobstructed geometry. The matrix of cross-section and longitudinal slopes used for the performance tests is provided in Table-2. To obtain a robust performance curve each combination of slopes used in conjunction with the CFI was subjected to 12 different input flows, from 1 cfs to 12 cfs. This flow is labeled “Gutter flow” in the performance curves. For each flow case an assessment of the self-cleaning velocity within CFI was made. Photos and video-recordings of the flows in the hydraulic model and at the exit from the CFI barrel were acquired for each performance test.

The hydraulics performance curves for the optimal design of the prototype CFI has been successfully tested under a variety of slope conditions. Using scale relationships, analysis and visualization tools final empirical relationships to predict the intercepted flow by the inlet have been developed. It is noted that there is not reference CFI geometry to compare the results in the present study, but previous results with similar geometry confirm that the obtained experimental data is in the expected range. In order to place the results in a better context the lines representing both 100% and 50% interception efficiency have been added to the performance curves. Use of the graphs is self-explanatory: for a known value of the flow in the gutter approaching the CFI (labeled gutter flow in the horizontal axis) use the performance curve to determine the flow intercepted by the drainage structure. The difference between the gutter flow and the intercepted flow quantifies the amount of stormwater bypassing the structure.

The main study results, the hydraulic performance curves, are plotted in Figures 23 to 28. Besides the raw data curves, each individual performance curve was also plotted as obtained by applying regression lines to the experimental points. During the initial stages of the data analysis, the experimental data was fit second order polynomial and logarithmic regression fits using Microsoft’s Excel software. Figure-23 illustrates the differences between the two regression line options applied to one of the experimental datasets. Based on the visualization results, it was decided to adopt the logarithmic regression for the illustration of the final results of this study. For clarity of the illustrations, only the regression curves are only plotted in Figures 24 to 28.

The corresponding raw experimental results are tabulated in Appendix C grouped by individual tests.

a)



b)

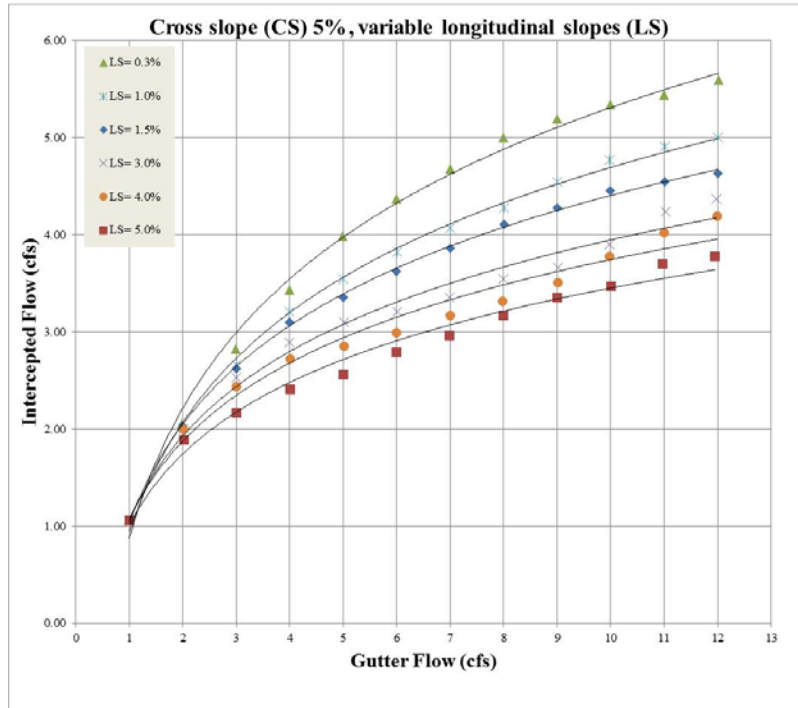


Figure 23: Comparison between regression fits applied to the raw experimental data: a) second order polynomial, and b) logarithmic

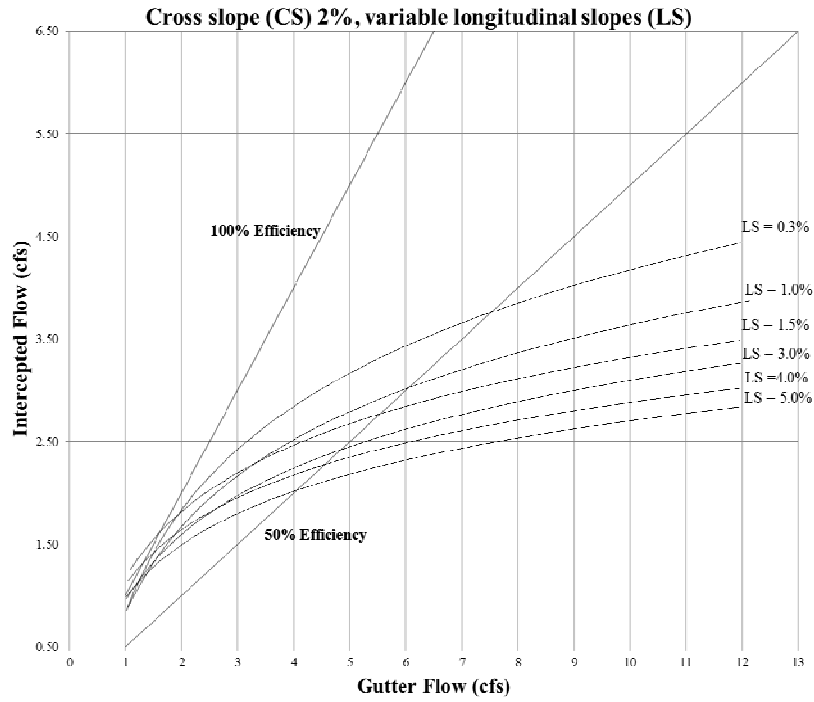


Figure 24: Hydraulic performance for 4-ft, 2% cross-slope CFI (all longitudinal slopes)

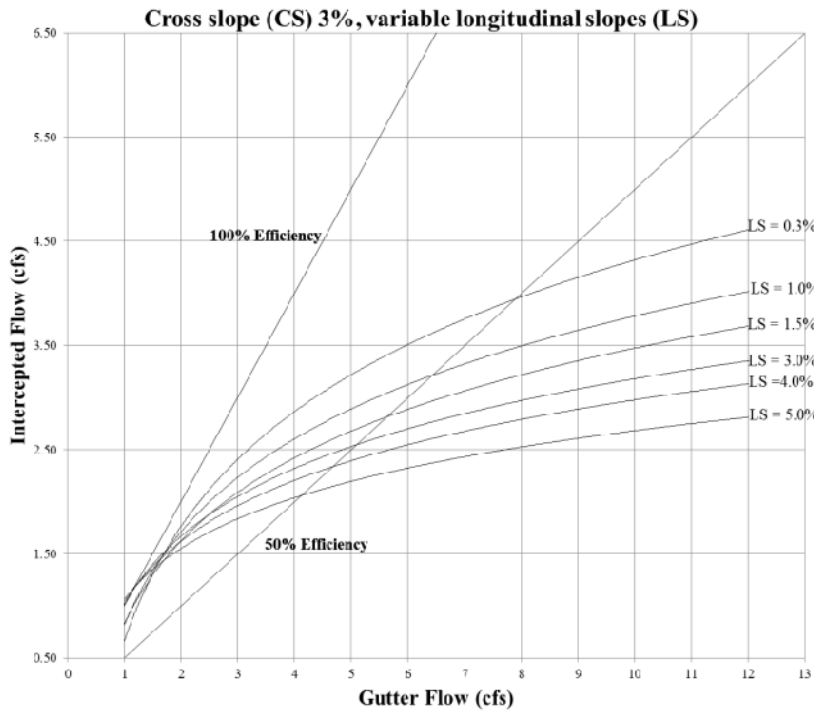


Figure 25: Hydraulic performance for 4-ft, 3% cross-slope CFI (all longitudinal slopes)

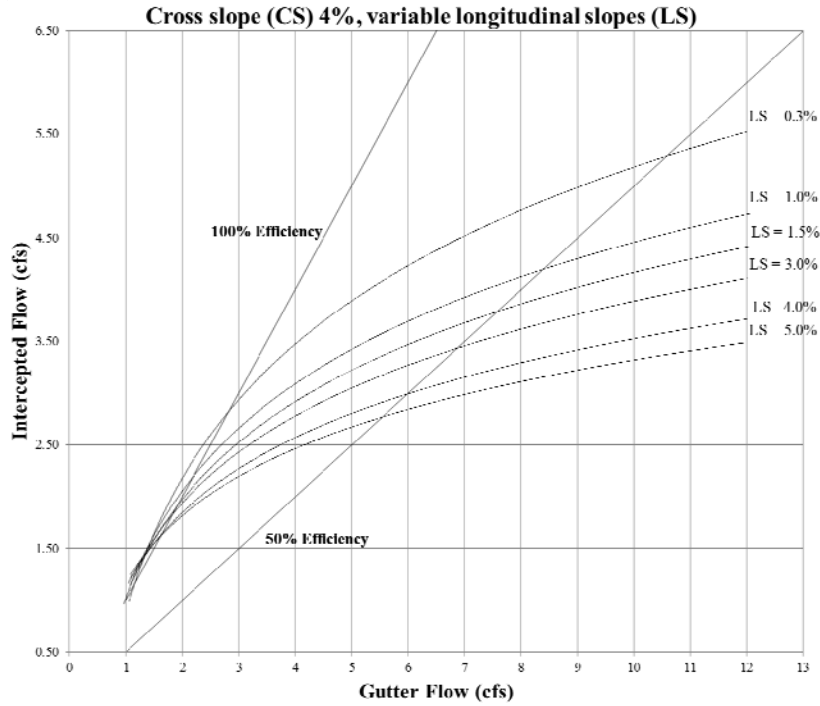


Figure 26: Hydraulic performance for 4-ft, 4% cross-slope CFI (all longitudinal slopes)

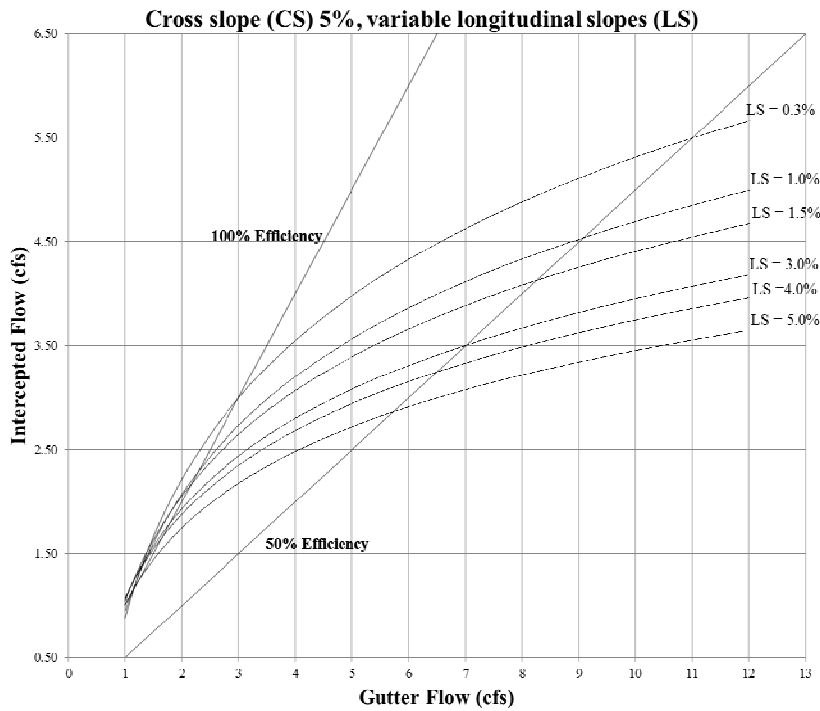


Figure 27: Hydraulic performance for 4-ft, 5% cross-slope CFI (all longitudinal slopes)

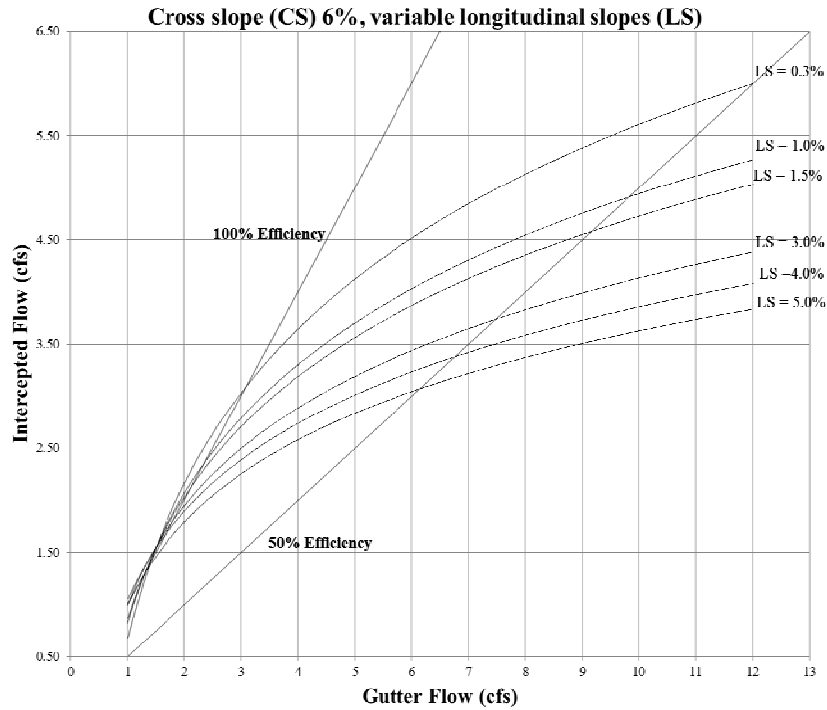


Figure 28: Hydraulic performance for 4-ft, 6% cross-slope CFI (all longitudinal slopes)

5.2.2 Discussion

Table 4 displays CFI mean velocities for the lowest flows tested in the model. All of these velocities are above the self-cleaning velocity of 2fts, hence the debris clogging is not expected for neither of the tested cases.

Table 4: Mean velocity over the CFI for selected low flow cases

5% LS	Q intercepted [cfs]	Exit Velocity [ft/s]
2%	1.08	5.49
	1.97	5.32
	2.35	5.45
	2.66	7.52
3%	1.02	4.82
	2.38	6.98
	2.66	7.31
	3.47	10.42
4%	1.16	7.29
	2.38	7.48
	3.07	10.14
	3.32	12.46
5%	1.06	12.41
	2.00	12.80
	2.17	13.05
	2.41	13.11
6%	1.00	12.59
	1.95	12.85
	2.32	13.42
	2.44	13.15

The performance curves plotted in Figures 23 to 28 illustrate several notable trends in the experimental data. First, as expected the increase in the cross-slope conveyed more stormwater toward the structure. Also expected was the trend of the data substantiating that the flatter the longitudinal slope, the larger the flow captured by the structure for the same cross-slope. The second trend was explained by the increased dynamic head of the approaching flow for large longitudinal slopes, thereby increasing the velocity of the flow approaching the drainage structure. Overall, it can be concluded that there was a modest increase in the efficiency of the inlet with the increased cross slope and a sharp decrease with the increase of the longitudinal slope. The latter conclusion is well supported by the alternative display of the data in Figures 29 to 34 whereby the datasets are grouped around the longitudinal slopes with cross slopes as parameters. An illustration of the trends in the variation of the maximum and minimum intercepted flows with the cross-slope and longitudinal slope variation is provided in Figure 35.

The CFI tested here (Index 216 FDOT, 2014 – see Appendix A) resembles closely in the upper part the Standard type 5 inlet (Index 211; FDOT 2014 – see Appendix B). A comparison of the results for Index 216 presented in this study with those of Index 211 illustrated in FDOT's Drainage Handbook is made in Figure-36. Overall, the results for our study show more than 1 cfs less intercepted flow for a gutter flow of 10 cfs. The results seem to be realistic given that the CFI tested in this study has a longer barrel than Type 5 inlet and does not have a grated opening.

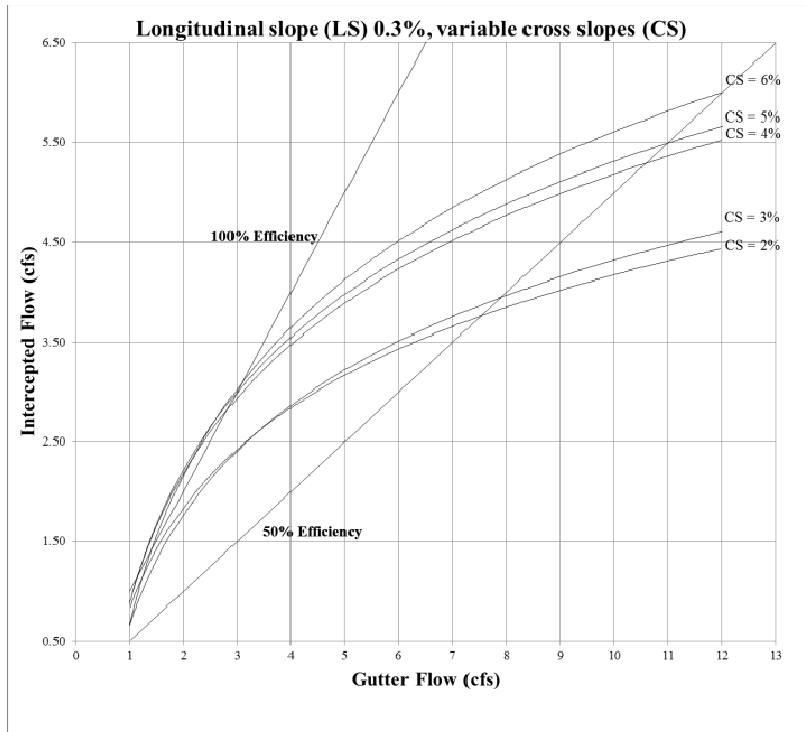


Figure 29: Hydraulic performance for 4-ft, 0.3% longitudinal slope CFI (all cross slopes)

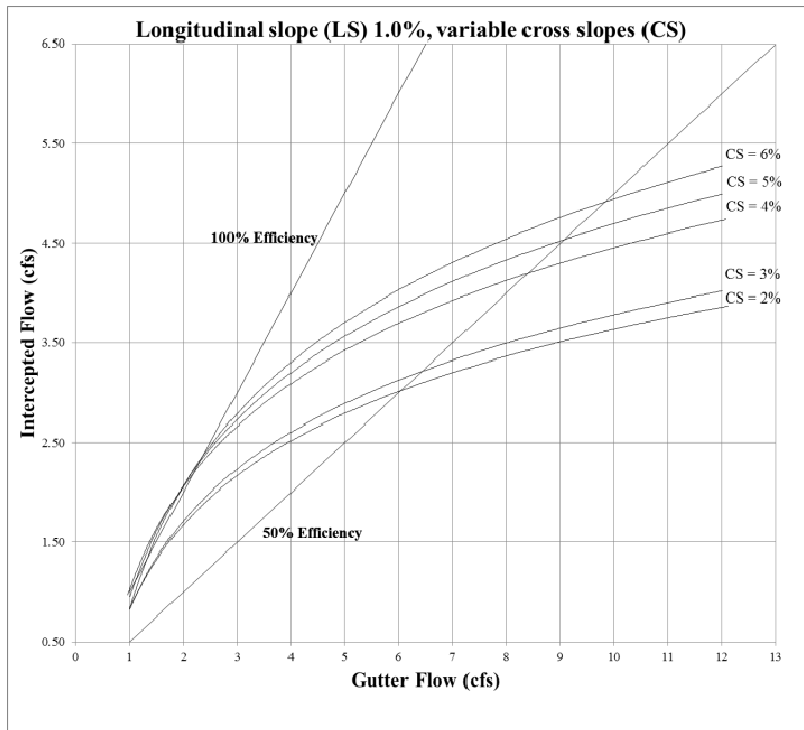


Figure 30: Hydraulic performance for 4-ft, 1.0% longitudinal slope CFI (all cross slopes)

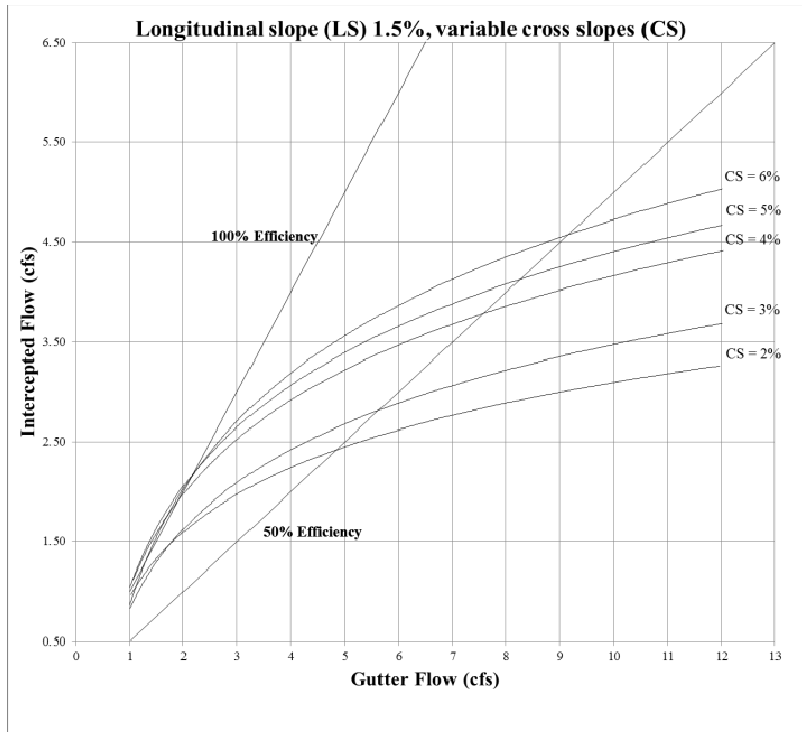


Figure 31: Hydraulic performance for 4-ft, 1.5% longitudinal slope CFI (all cross slopes)

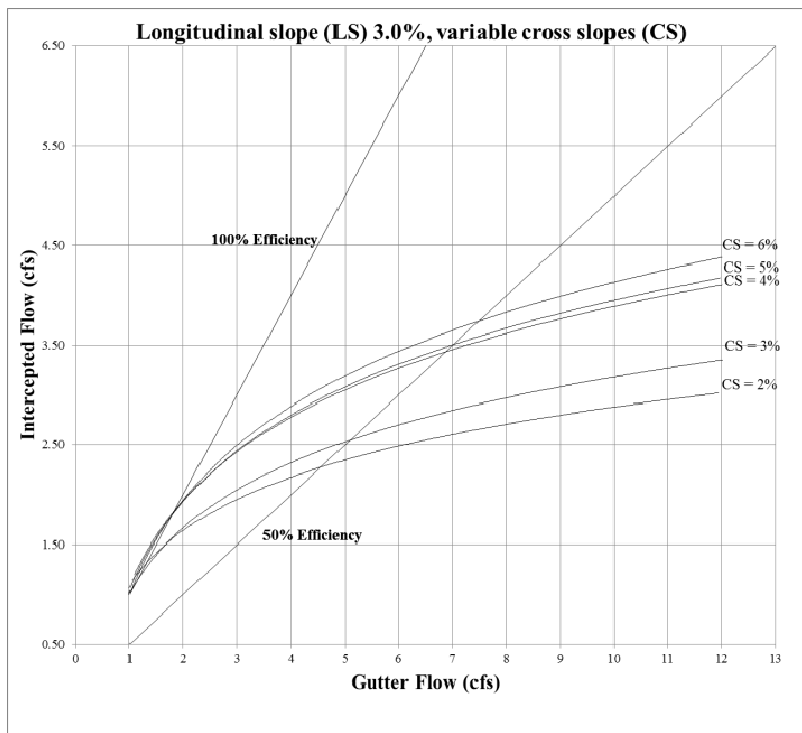


Figure 32: Hydraulic performance for 4-ft, 3.0% longitudinal slope CFI (all cross slopes)

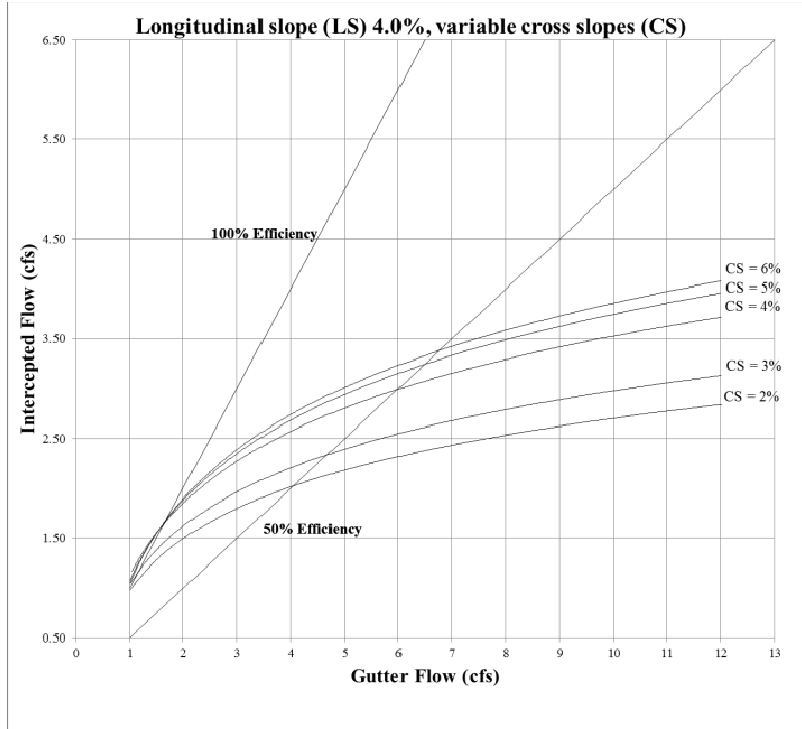


Figure 33: Hydraulic performance for 4-ft, 4.0% longitudinal slope CFI (all cross slopes)

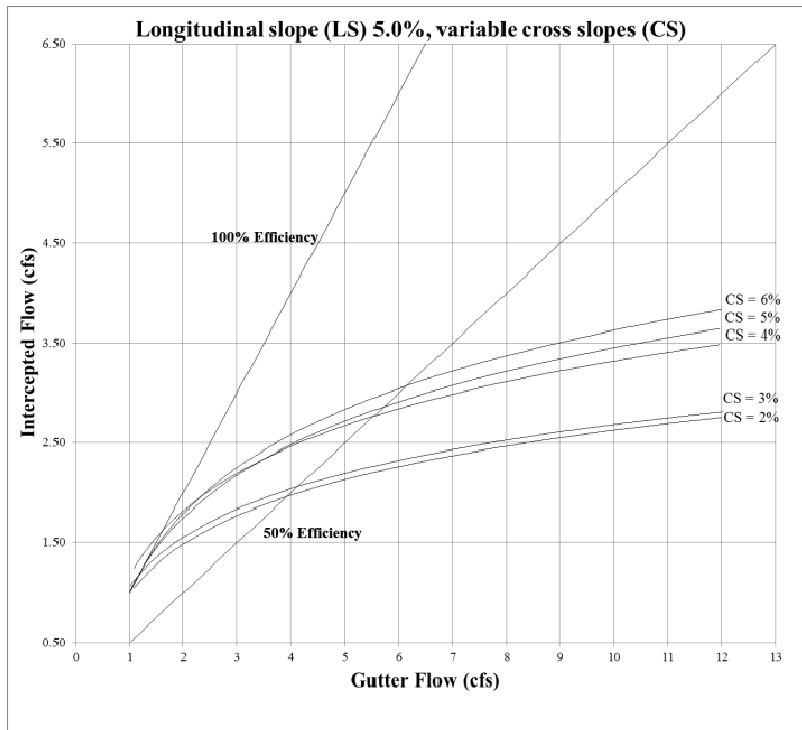


Figure 34: Hydraulic performance for 4-ft, 5.0% longitudinal slope CFI (all cross slopes)

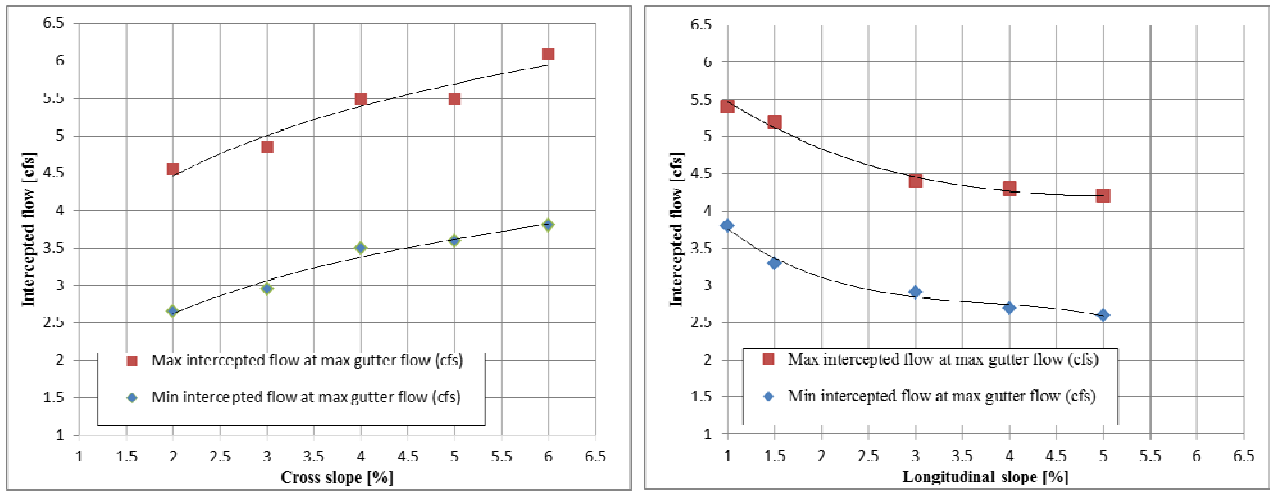
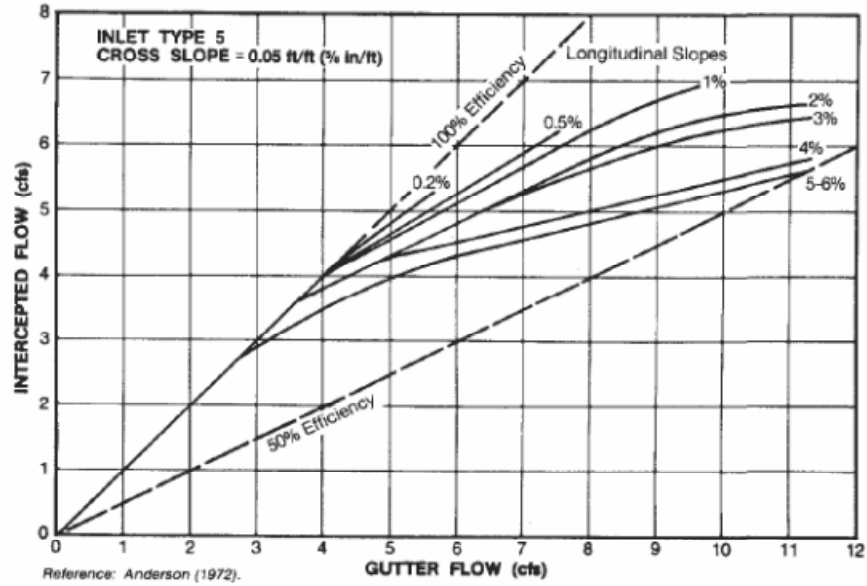


Figure 35: Trends in the variation of the maximum and minimum diverted flows with the change in the cross and longitudinal slopes

a)



b)

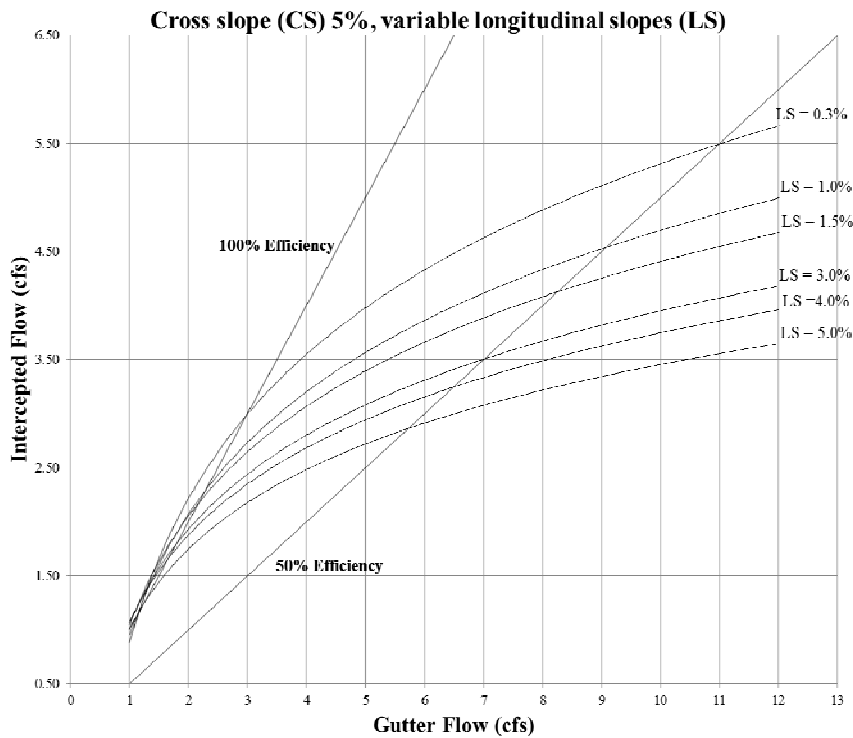


Figure 36: Comparison of the hydraulic performance curve for: a) Index 211 CFI type 5 (FDOT, 2014), and b) Index 216 CFI (tested in the present study)

6. CONCLUSIONS

The flow through drainage structures is complex and cannot be easily modeled by simulations or investigated analytically to establish their hydraulic efficiency in flow interception. Most of the current design practice is based upon empirical formulas obtained through laboratory tests. The current study investigates the hydraulic efficiency of a modified closed flume inlet designed by the Florida Department of Transportation. Specifically, this study provides design details on the hydraulic efficiency of Index 216 Closed flume inlet (FDOT, 2014).

The experimental results presented in the study cover a wide range of flows (from 1 to 12 cfs), cross-slopes (from 2% to 6%) and longitudinal slopes (from 0.3% to 5%). The trends in the hydraulic performance of the drainage structure are aligned with the analytical expectation:

- increased cross slopes convey more stormwater through the drainage structure for the same longitudinal slope
- decreased longitudinal slopes convey more flow through the drainage for the same cross slope.

The efficiency of the drainage structures for larger cross-slope is modest while a sharp decrease occurs for larger longitudinal slopes. The results of the hydraulic model presented in this study provide a baseline for designers of closed flume inlets by setting more definitive guidelines for inlet manufacturers to follow.

REFERENCES

- Anderson, M.W. (1972). *A Study of Storm-water Inlet Capacities*. Report for Florida Department of Transportation, University of South Florida, Tampa, FL.
- Bauer, W.J., and Woo, D-C. (1964). *Hydraulic Design of Depressed Curb-opening Inlets* Research report No. 58, Highway Research Board, Washington, D.C.
- Conner, N.W. (1945). "Design and Capacity of Gutter Inlets." Proceedings Highway Research Board, Vol. 25, Washington, D.C.
- FDOT (2012). "Drainage Handbook – Storm Drains." Office of Design, Florida Department of Transportation, Tallahassee, FL.
<<http://www.dot.state.fl.us/rddesign/dr/files/StormDrainHB.pdf> >.
- FDOT (2014). "Design Standards eBooklet 2014." Florida Department of Transportation," Tallahassee, FL <<http://www.dot.state.fl.us/rddesign/DS/14/STDs.shtm>>.
- Guo, J.C.Y. and MacKenzie, K. (2012). "Hydraulic Efficiency of Grate and Curb-opening Inlets under Clogging Effect." Report No. CDOT-2-12-3, University of Colorado, Denver, CO.
- Hydraulic Institute Standards (1998). "American National Standard for Pump Intake Design." ANSI/HI 9.8-1998, Parsippany, NJ.
- Izzard, C.F. (1950). "Tentative Results on Capacity of Curb Opening Inlets." Research Report no. 11-B. Highway Research Board, Washington, DC.
- Johnson, F.L. and Chang, F.M. (1984). "Drainage of Highway Pavements HEC12." Federal Highway Administration (FHWA), McLean, Virginia.
<<http://www.fhwa.dot.gov/engineering/hydraulics/pubs/hec/hec12.pdf>>
- Kranc, S.C. (1998). "Hydraulic Performance of Drainage Structures, Phase I and II." Report No. 790 for Florida Department of Transportation, University of South Florida, Tampa, FL.
- Li, W.H., Goodell, B.C., and Heyer, J.C. (1954). "Flow into Depressed Combination Inlets." Journal of Sewage and Industrial Wastes, Vol. 26 (8), p. 967.
- Mays W. L. (2010) "Water Resources Engineering", John Wiley & Sons Inc., NJ.
- USACE (1949). "Surface Drainage facilities for Airfields." Engineering Manual, Part XIII, Ch. 1. U.S. Corps of Engineers.
- Water Measurement Manual. United States Department of the Interior, Bureau of Reclamation, Revised Reprint, 2001.

Wintz, W.A. and Kuo, Y. (1969). "A Study of Storm-water Inlet Capacities." Report No. 736-00-69 for the Louisiana Department of Highways, Louisiana State University, Baton Rouge, LA.

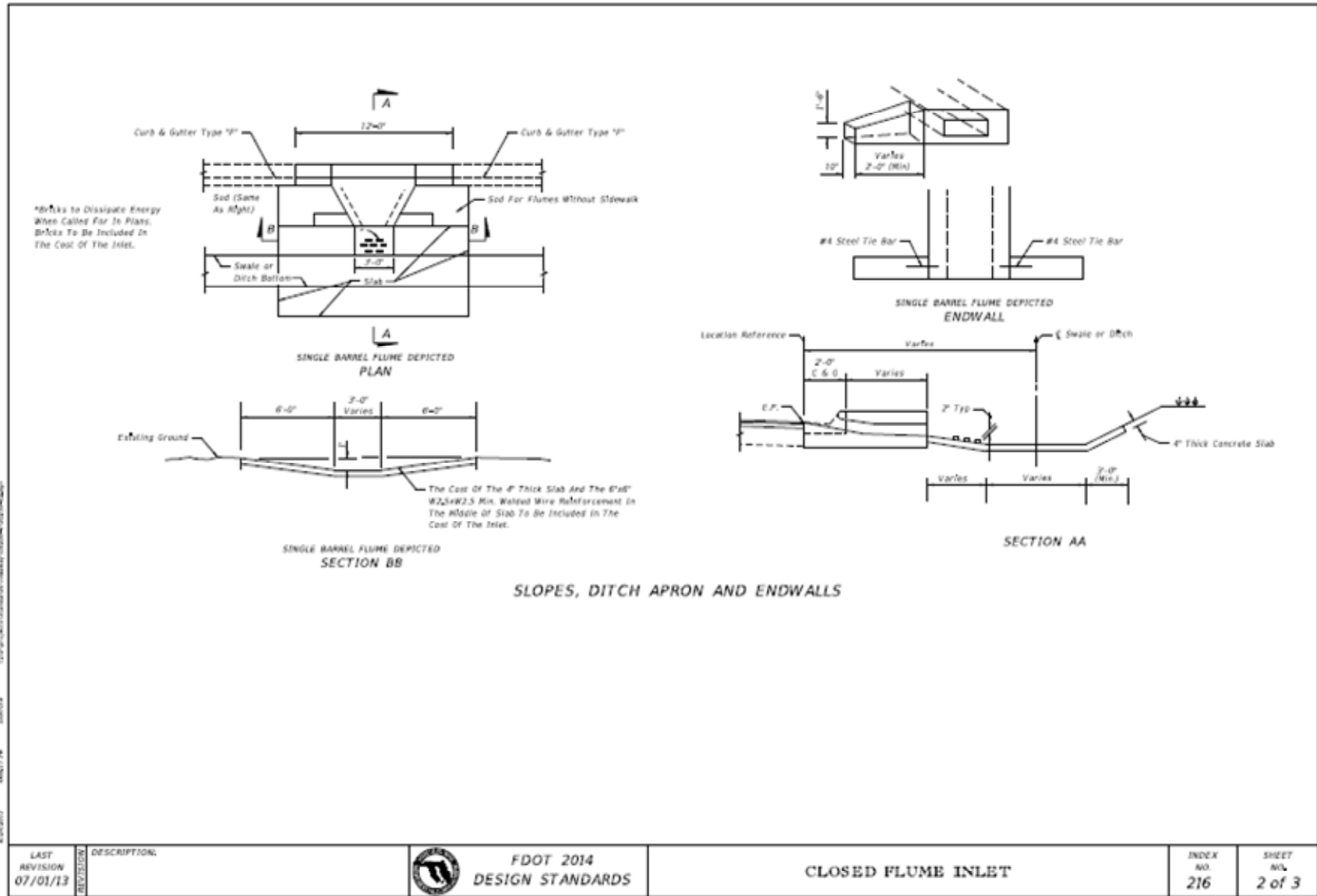


Figure A: FDOT 2014 design standards-closed flume inlet-index 216 (Part 2)

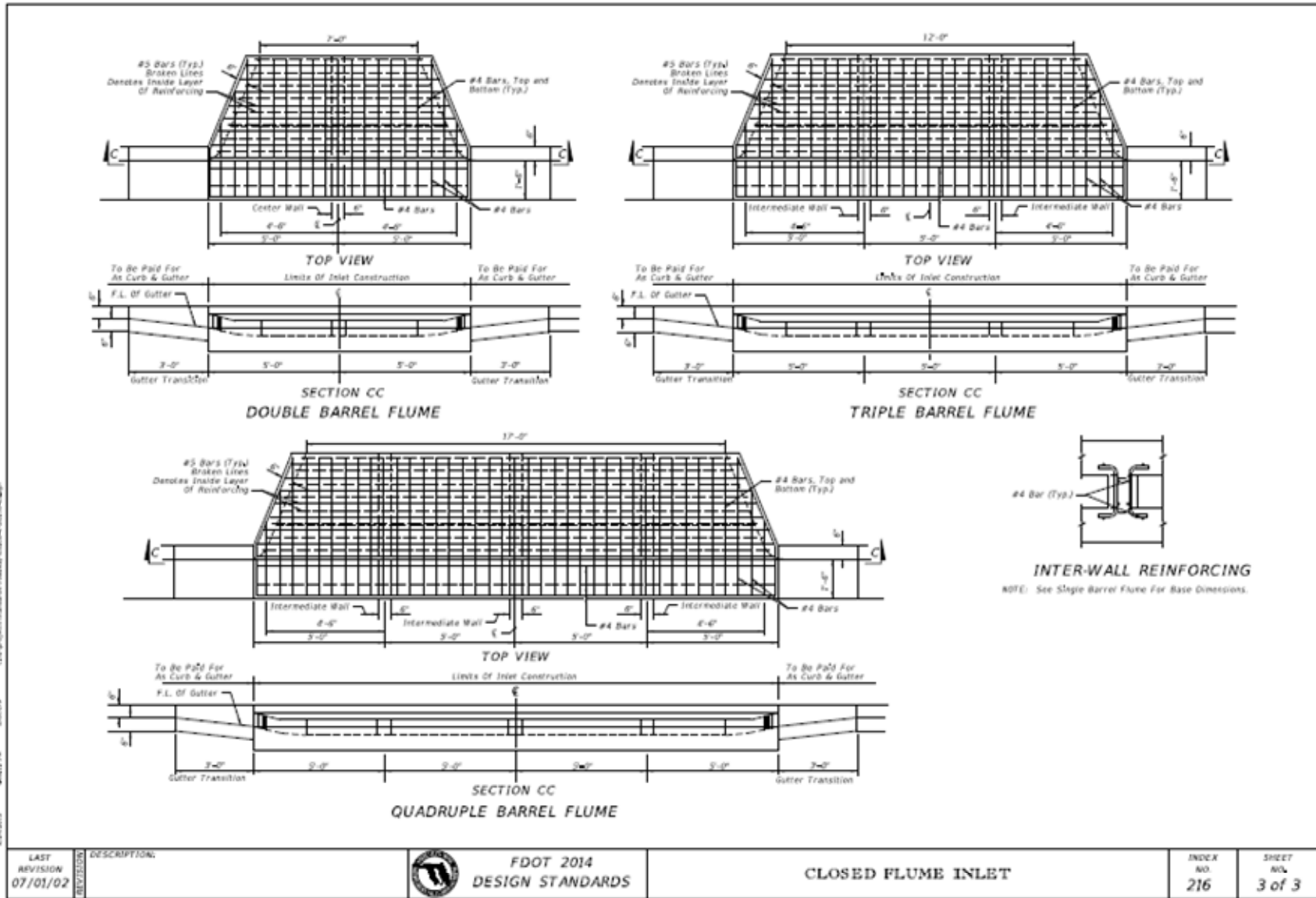


Figure A: FDOT 2014 design standards-closed flume inlet-index 216 (Part 3)

APPENDIX B CFI Type 5 and 6

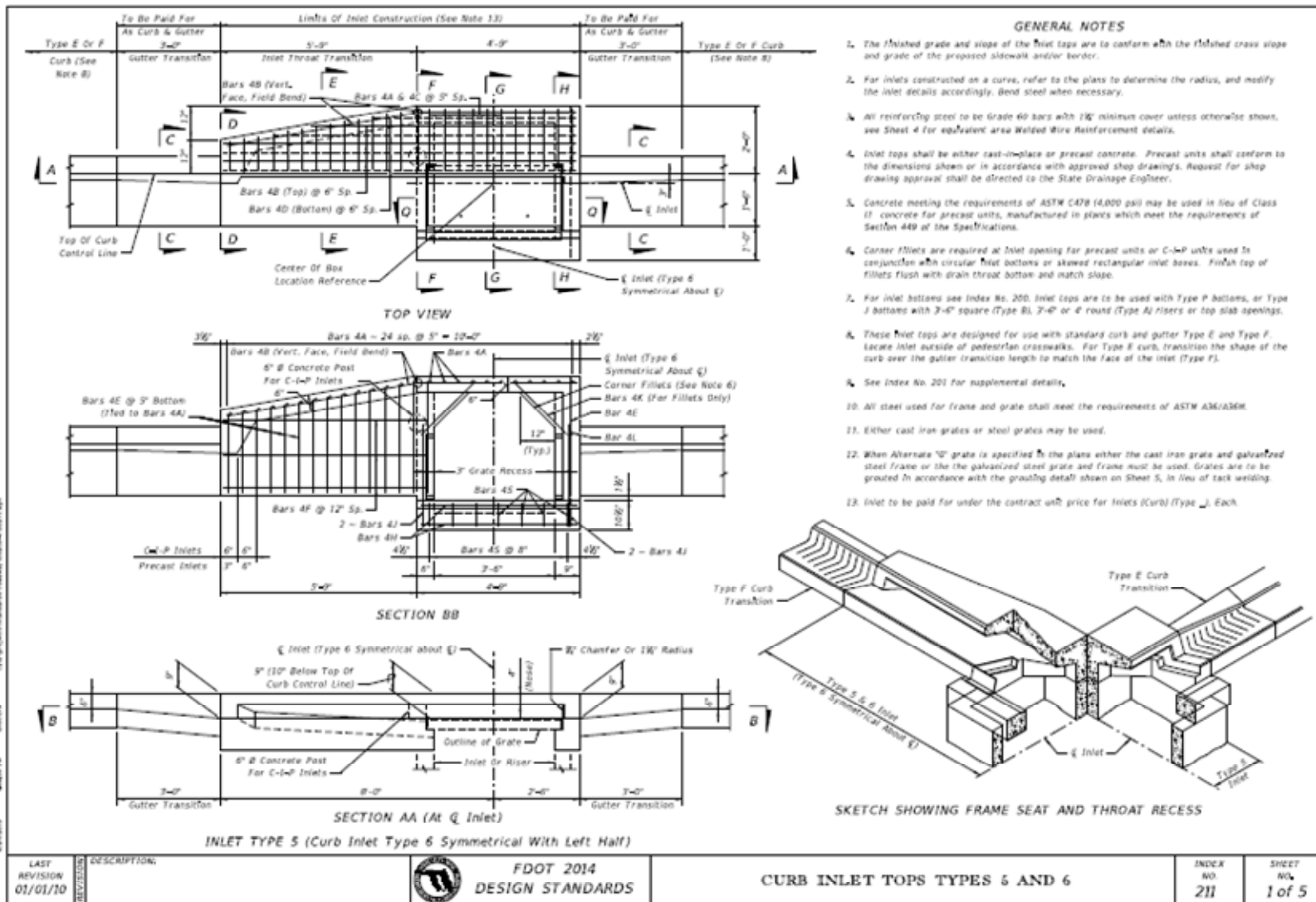


Figure B: FDOT 2014 design standards-curb inlet tops types 5 and 6 (Part 1)

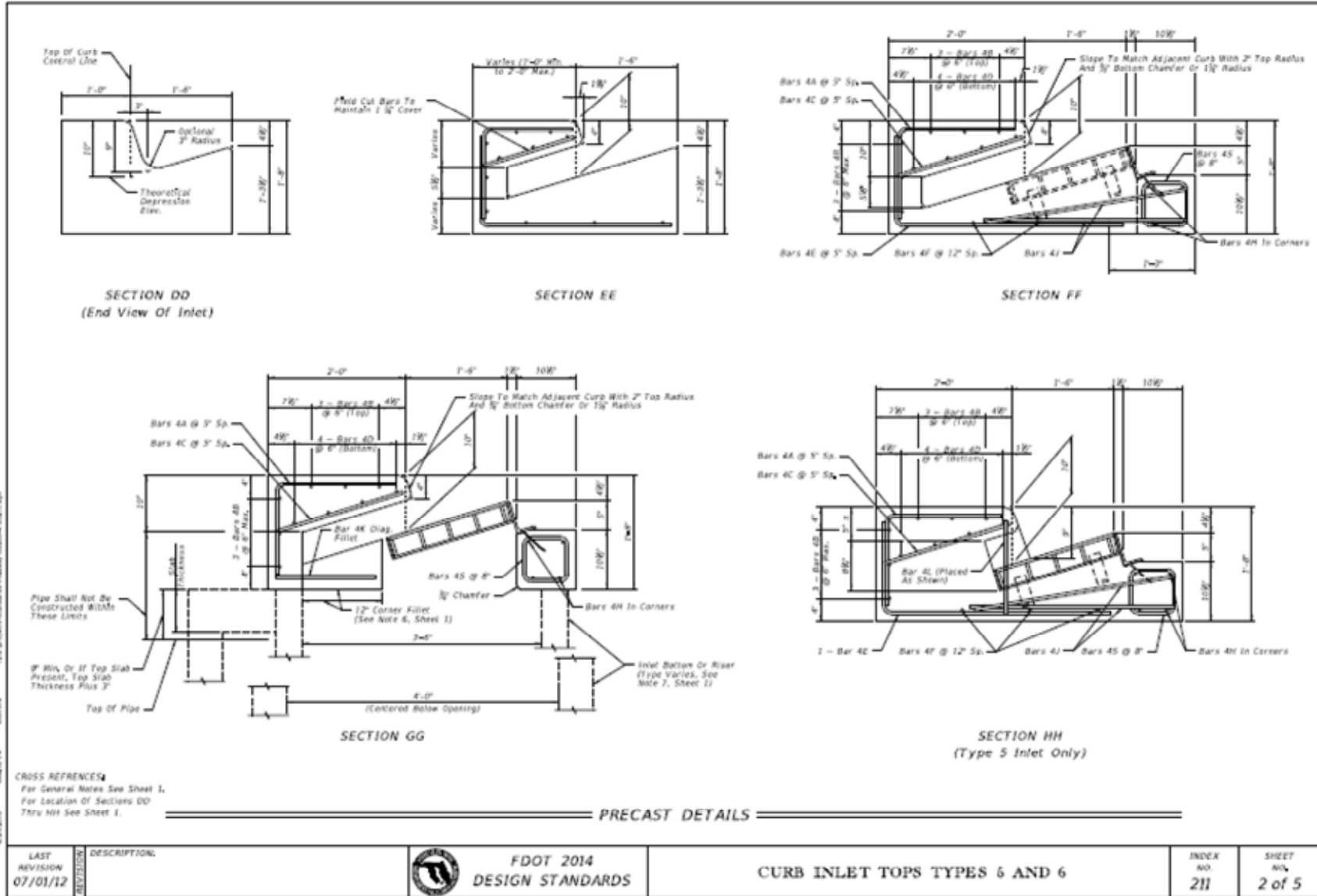
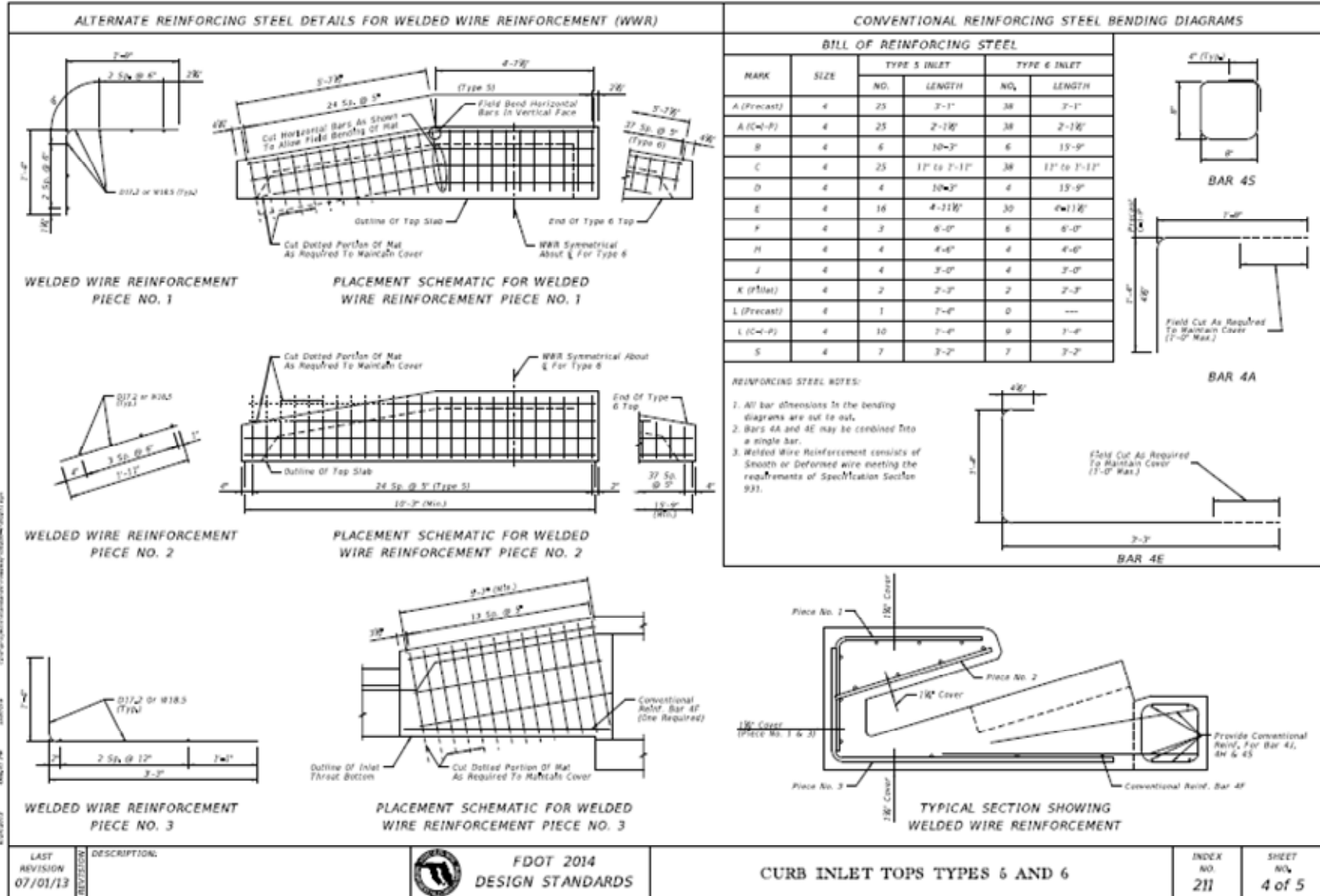


Figure B: FDOT 2014 design standards-curb inlet tops types 5 and 6 (Part 2)



**TYPICAL SECTION SHOWING
WELDED WIRE REINFORCEMENT**

Figure B: FDOT 2014 design standards-curb inlet tops types 5 and 6 (Part 4)

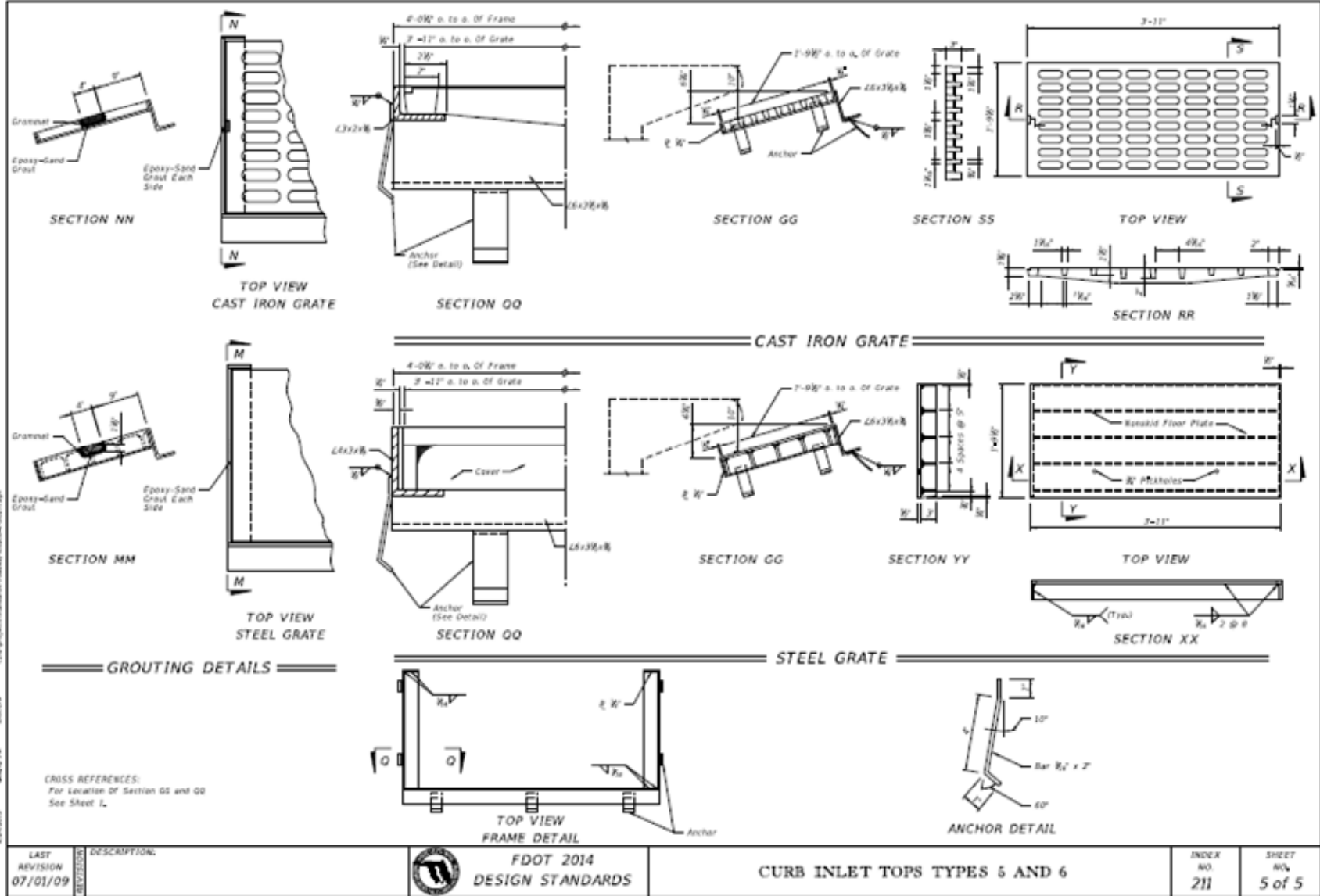


Figure B: FDOT 2014 design standards-curb inlet tops types 5 and 6 (Part 5)

APPENDIX C Numerical Results

Table C: Numerical results of experiments

Configuration	Incoming gutter flow		Q Actual		Intercepted flow		
	Q _{Gutter} (cfs)	Q (gpm - m)		cfs	Pt Gage _{V-notch} (ft)	H _{V-notch} (ft)	Q _{CFI} (cfs)
-0.3% Longitudinal Slope - 6% Cross Slope	1.0	8.03	8.04	1.00	0.994	0.142	1.06
	2.0	16.06	16.00	1.99	1.035	0.183	2.00
	3.0	24.09	24.08	3.00	1.061	0.209	2.79
	4.0	32.12	32.10	4.00	1.08	0.228	3.47
	5.0	40.14	40.20	5.01	1.092	0.240	3.94
	6.0	48.17	48.08	5.99	1.102	0.250	4.37
	7.0	56.20	56.01	6.98	1.112	0.260	4.82
	8.0	64.23	64.28	8.01	1.121	0.269	5.25
	9.0	72.26	72.22	8.99	1.125	0.273	5.44
	10.0	80.29	80.38	10.01	1.13	0.278	5.69
	11.0	88.32	88.40	11.01	1.135	0.283	5.95
	12.0	96.35	96.30	11.99	1.138	0.286	6.11
- 1.0% Longitudinal Slope - 6% Cross Slope	1.0	8.03	8.02	1.00	0.993	0.141	1.04
	2.0	16.06	16.08	2.00	1.035	0.183	2.00
	3.0	24.09	24.08	3.00	1.058	0.206	2.69
	4.0	32.12	32.10	4.00	1.074	0.222	3.25
	5.0	40.14	40.15	5.00	1.083	0.231	3.58
	6.0	48.17	48.24	6.01	1.092	0.240	3.94
	7.0	56.20	56.22	7.00	1.097	0.245	4.15
	8.0	64.23	64.16	7.99	1.104	0.252	4.46
	9.0	72.26	72.22	8.99	1.111	0.259	4.77
	10.0	80.29	80.26	10.00	1.117	0.265	5.05
	11.0	88.32	88.26	10.99	1.121	0.269	5.25
	12.0	96.35	96.42	12.01	1.125	0.273	5.44

Table C: Numerical results of experiments (continued)

Configuration	Incoming gutter flow		Q Actual		Intercepted flow		
	Q _{Gutter} (cfs)	Q (gpm - m)		cfs	Pt Gage _{V-notch} (ft)	H _{V-notch} (ft)	Q _{CFI} (cfs)
- 1.5% Longitudinal Slope - 6% Cross Slope	1.0	8.03	8.04	1.00	0.994	0.142	1.06
	2.0	16.06	16.03	2.00	1.036	0.184	2.03
	3.0	24.09	24.08	3.00	1.054	0.202	2.56
	4.0	32.12	32.10	4.00	1.071	0.219	3.14
	5.0	40.14	40.15	5.00	1.079	0.227	3.43
	6.0	48.17	48.20	6.00	1.085	0.233	3.66
	7.0	56.20	56.30	7.01	1.092	0.240	3.94
	8.0	64.23	64.16	7.99	1.100	0.248	4.28
	9.0	72.26	72.34	9.01	1.107	0.255	4.59
	10.0	80.29	80.26	10.00	1.113	0.261	4.86
	11.0	88.32	88.26	10.99	1.117	0.265	5.05
	12.0	96.35	96.42	12.01	1.119	0.267	5.15
-3% Longitudinal Slope - 6% Cross Slope	1.0	8.03	8.00	1.00	0.994	0.142	1.06
	2.0	16.06	16.08	2.00	1.034	0.182	1.97
	3.0	24.09	24.08	3.00	1.049	0.197	2.41
	4.0	32.12	32.22	4.01	1.068	0.216	3.03
	5.0	40.14	40.20	5.01	1.075	0.223	3.28
	6.0	48.17	48.21	6.00	1.077	0.225	3.36
	7.0	56.20	56.22	7.00	1.08	0.228	3.47
	8.0	64.23	64.34	8.01	1.082	0.230	3.55
	9.0	72.26	72.34	9.01	1.084	0.232	3.62
	10.0	80.29	80.28	10.00	1.090	0.238	3.86
	11.0	88.32	88.40	11.01	1.097	0.245	4.15
	12.0	96.35	96.42	12.01	1.102	0.250	4.37

Table C: Numerical results of experiments (continued)

Configuration	Incoming gutter flow		Q Actual		Intercepted flow		
	Q _{Gutter} (cfs)	Q (gpm - m)		cfs	Pt Gage _{V-notch} (ft)	H _{V-notch} (ft)	Q _{CFI} (cfs)
- 4% Longitudinal Slope - 6% Cross Slope	1.0	8.03	8.08	1.01	0.994	0.142	1.06
	2.0	16.06	15.88	1.98	1.033	0.181	1.95
	3.0	24.09	24.09	3.00	1.052	0.200	2.50
	4.0	32.12	32.46	4.04	1.064	0.212	2.89
	5.0	40.14	40.14	5.00	1.068	0.216	3.03
	6.0	48.17	48.45	6.03	1.070	0.218	3.10
	7.0	56.20	56.34	7.02	1.073	0.221	3.21
	8.0	64.23	64.28	8.01	1.076	0.224	3.32
	9.0	72.26	72.34	9.01	1.082	0.230	3.55
	10.0	80.29	80.14	9.98	1.088	0.236	3.78
	11.0	88.32	88.41	11.01	1.095	0.243	4.07
	12.0	96.35	96.42	12.01	1.100	0.248	4.28
- 5% Longitudinal Slope - 6% Cross Slope	1.0	8.03	8.04	1.00	0.994	0.142	1.06
	2.0	16.06	15.90	1.98	1.033	0.181	1.95
	3.0	24.09	24.08	3.00	1.046	0.194	2.32
	4.0	32.12	32.30	4.02	1.050	0.198	2.44
	5.0	40.14	40.14	5.00	1.054	0.202	2.56
	6.0	48.17	48.22	6.01	1.058	0.206	2.69
	7.0	56.20	56.22	7.00	1.064	0.212	2.89
	8.0	64.23	64.30	8.01	1.072	0.220	3.17
	9.0	72.26	72.10	8.98	1.078	0.226	3.39
	10.0	80.29	80.38	10.01	1.086	0.234	3.70
	11.0	88.32	88.40	11.01	1.093	0.241	3.98
	12.0	96.35	96.30	11.99	1.097	0.245	4.15

Table C: Numerical results of experiments (continued)

Configuration	Incoming gutter flow		Q Actual		Intercepted flow		
	Q _{Gutter} (cfs)	Q (gpm - m)		cfs	Pt Gage _{V-notch} (ft)	H _{V-notch} (ft)	Q _{CFI} (cfs)
-0.3% Longitudinal Slope - 5% Cross Slope	1.0	8.03	8.00	1.00	0.994	0.142	1.06
	2.0	16.06	15.97	1.99	1.037	0.185	2.06
	3.0	24.09	23.96	2.98	1.062	0.210	2.82
	4.0	32.12	32.10	4.00	1.079	0.227	3.43
	5.0	40.14	40.03	4.99	1.093	0.241	3.98
	6.0	48.17	48.10	5.99	1.102	0.250	4.37
	7.0	56.20	56.22	7.00	1.109	0.257	4.68
	8.0	64.23	64.20	8.00	1.116	0.264	5.00
	9.0	72.26	72.22	8.99	1.120	0.268	5.20
	10.0	80.29	80.26	10.00	1.123	0.271	5.34
	11.0	88.32	88.30	11.00	1.125	0.273	5.44
	12.0	96.35	96.52	12.02	1.128	0.276	5.59
- 1.0% Longitudinal Slope - 5% Cross Slope	1.0	8.03	8.08	1.01	0.994	0.142	1.06
	2.0	16.06	16.10	2.01	1.035	0.183	2.00
	3.0	24.09	24.08	3.00	1.057	0.205	2.66
	4.0	32.12	32.10	4.00	1.073	0.221	3.21
	5.0	40.14	40.15	5.00	1.082	0.230	3.55
	6.0	48.17	48.20	6.00	1.089	0.237	3.82
	7.0	56.20	56.22	7.00	1.095	0.243	4.07
	8.0	64.23	64.25	8.00	1.1	0.248	4.28
	9.0	72.26	72.22	8.99	1.106	0.254	4.54
	10.0	80.29	80.15	9.98	1.111	0.259	4.77
	11.0	88.32	88.40	11.01	1.114	0.262	4.91
	12.0	96.35	96.40	12.01	1.116	0.264	5.00

Table C: Numerical results of experiments (continued)

Configuration	Incoming gutter flow		Q Actual		Intercepted flow		
	Q _{Gutter} (cfs)	Q (gpm - m)		cfs	Pt Gage _{V-notch} (ft)	H _{V-notch} (ft)	Q _{CFI} (cfs)
- 1.5% Longitudinal Slope - 5% Cross Slope	1.0	8.03	8.04	1.00	0.994	0.142	1.06
	2.0	16.06	16.00	1.99	1.036	0.184	2.03
	3.0	24.09	24.08	3.00	1.056	0.204	2.63
	4.0	32.12	32.10	4.00	1.070	0.218	3.10
	5.0	40.14	40.14	5.00	1.077	0.225	3.36
	6.0	48.17	48.09	5.99	1.084	0.232	3.62
	7.0	56.20	56.22	7.00	1.090	0.238	3.86
	8.0	64.23	64.28	8.01	1.096	0.244	4.11
	9.0	72.26	72.22	8.99	1.100	0.248	4.28
	10.0	80.29	80.26	10.00	1.104	0.252	4.46
	11.0	88.32	88.40	11.01	1.106	0.254	4.54
	12.0	96.35	96.40	12.01	1.108	0.256	4.63
-3% Longitudinal Slope - 5% Cross Slope	1.0	8.03	8.04	1.00	0.993	0.141	1.04
	2.0	16.06	16.05	2.00	1.036	0.184	2.03
	3.0	24.09	24.08	3.00	1.054	0.202	2.56
	4.0	32.12	32.10	4.00	1.066	0.214	2.96
	5.0	40.14	40.26	5.01	1.069	0.217	3.07
	6.0	48.17	48.21	6.00	1.070	0.218	3.10
	7.0	56.20	56.10	6.99	1.072	0.220	3.17
	8.0	64.23	64.16	7.99	1.075	0.223	3.28
	9.0	72.26	72.34	9.01	1.082	0.230	3.55
	10.0	80.29	80.14	9.98	1.090	0.238	3.86
	11.0	88.32	88.50	11.02	1.099	0.247	4.24
	12.0	96.35	96.18	11.98	1.102	0.250	4.37

Table C: Numerical results of experiments (continued)

Configuration	Incoming gutter flow		Q Actual		Intercepted flow		
	Q _{Gutter} (cfs)	Q (gpm - m)		cfs	Pt Gage _{v-notch} (ft)	H _{v-notch} (ft)	Q _{CFI} (cfs)
- 4% Longitudinal Slope - 5% Cross Slope	1.0	8.03	8.07	1.01	0.994	0.142	1.06
	2.0	16.06	16.10	2.01	1.035	0.183	2.00
	3.0	24.09	24.08	3.00	1.054	0.202	2.56
	4.0	32.12	32.22	4.01	1.059	0.207	2.72
	5.0	40.14	40.26	5.01	1.062	0.210	2.82
	6.0	48.17	48.14	6.00	1.066	0.214	2.96
	7.0	56.20	56.22	7.00	1.069	0.217	3.07
	8.0	64.23	64.10	7.98	1.073	0.221	3.21
	9.0	72.26	72.34	9.01	1.080	0.228	3.47
	10.0	80.29	80.14	9.98	1.088	0.236	3.78
	11.0	88.32	88.28	11.00	1.094	0.242	4.03
	12.0	96.35	96.30	11.99	1.098	0.246	4.19
- 5% Longitudinal Slope - 5% Cross Slope	1.0	8.03	8.04	1.00	0.994	0.142	1.06
	2.0	16.06	16.26	2.03	1.035	0.183	2.00
	3.0	24.09	24.08	3.00	1.041	0.189	2.17
	4.0	32.12	32.22	4.01	1.049	0.197	2.41
	5.0	40.14	40.14	5.00	1.054	0.202	2.56
	6.0	48.17	48.10	5.99	1.061	0.209	2.79
	7.0	56.20	56.08	6.98	1.066	0.214	2.96
	8.0	64.23	64.15	7.99	1.072	0.220	3.17
	9.0	72.26	72.31	9.01	1.077	0.225	3.36
	10.0	80.29	80.38	10.01	1.08	0.228	3.47
	11.0	88.32	88.05	10.97	1.086	0.234	3.70
	12.0	96.35	96.00	11.96	1.088	0.236	3.78

Table C: Numerical results of experiments (continued)

Configuration	Incoming gutter flow		Q Actual		Intercepted flow		
	Q _{Gutter} (cfs)	Q (gpm - m)		cfs	Pt Gage _{V-notch} (ft)	H _{V-notch} (ft)	Q _{CFI} (cfs)
-0.3% Longitudinal Slope - 4% Cross Slope	1.0	8.03	8.46	1.05	0.999	0.147	1.16
	2.0	16.06	16.78	2.09	1.041	0.189	2.17
	3.0	24.09	24.85	3.10	1.062	0.210	2.82
	4.0	32.12	32.44	4.04	1.078	0.226	3.39
	5.0	40.14	40.12	5.00	1.088	0.236	3.78
	6.0	48.17	48.35	6.02	1.1	0.248	4.28
	7.0	56.20	55.25	6.88	1.106	0.254	4.54
	8.0	64.23	64.06	7.98	1.114	0.262	4.91
	9.0	72.26	72.31	9.01	1.118	0.266	5.10
	10.0	80.29	79.68	9.92	1.121	0.269	5.25
	11.0	88.32	88.31	11.00	1.123	0.271	5.34
	12.0	96.35	90.42	11.26	1.129	0.277	5.64
- 1.0% Longitudinal Slope -4 % Cross Slope	1.0	8.03	7.74	0.96	0.995	0.143	1.08
	2.0	16.06	16.44	2.05	1.034	0.182	1.97
	3.0	24.09	24.70	3.08	1.055	0.203	2.59
	4.0	32.12	32.75	4.08	1.069	0.217	3.07
	5.0	40.14	40.82	5.08	1.08	0.228	3.47
	6.0	48.17	47.42	5.91	1.087	0.235	3.74
	7.0	56.20	56.06	6.98	1.093	0.241	3.98
	8.0	64.23	63.96	7.97	1.097	0.245	4.15
	9.0	72.26	71.76	8.94	1.101	0.249	4.32
	10.0	80.29	79.78	9.94	1.103	0.251	4.41
	11.0	88.32	89.33	11.13	1.105	0.253	4.50
	12.0	96.35	96.92	12.07	1.11	0.258	4.73

Table C: Numerical results of experiments (continued)

Configuration	Incoming gutter flow		Q Actual		Intercepted flow		
	Q _{Gutter} (cfs)	Q (gpm - m)		cfs	Pt Gage _{V-notch} (ft)	H _{V-notch} (ft)	Q _{CFI} (cfs)
- 1.5% Longitudinal Slope - 4% Cross Slope	1.0	8.03	8.58	1.07	0.998	0.146	1.14
	2.0	16.06	15.66	1.95	1.031	0.179	1.89
	3.0	24.09	23.48	2.92	1.051	0.199	2.47
	4.0	32.12	32.22	4.01	1.067	0.215	3.00
	5.0	40.14	40.72	5.07	1.076	0.224	3.32
	6.0	48.17	47.60	5.93	1.083	0.231	3.58
	7.0	56.20	56.01	6.98	1.087	0.235	3.74
	8.0	64.23	64.40	8.02	1.089	0.237	3.82
	9.0	72.26	71.90	8.96	1.093	0.241	3.98
	10.0	80.29	80.26	10.00	1.095	0.243	4.07
	11.0	88.32	87.52	10.90	1.1	0.248	4.28
	12.0	96.35	96.58	12.03	1.105	0.253	4.50
-3% Longitudinal Slope - 4% Cross Slope	1.0	8.03	8.70	1.08	0.997	0.145	1.12
	2.0	16.06	16.51	2.06	1.038	0.186	2.09
	3.0	24.09	25.10	3.13	1.056	0.204	2.63
	4.0	32.12	31.51	3.92	1.061	0.209	2.79
	5.0	40.14	39.65	4.94	1.064	0.212	2.89
	6.0	48.17	49.01	6.10	1.070	0.218	3.10
	7.0	56.20	56.52	7.04	1.074	0.222	3.25
	8.0	64.23	64.92	8.09	1.081	0.229	3.51
	9.0	72.26	72.41	9.02	1.087	0.235	3.74
	10.0	80.29	79.82	9.94	1.090	0.238	3.86
	11.0	88.32	88.24	10.99	1.094	0.242	4.03
	12.0	96.35	96.46	12.01	1.1	0.248	4.28

Table C: Numerical results of experiments (continued)

Configuration	Incoming gutter flow		Q Actual		Intercepted flow		
	Q _{Gutter} (cfs)	Q (gpm - m)		cfs	Pt Gage _{V-notch} (ft)	H _{V-notch} (ft)	Q _{CFI} (cfs)
- 4% Longitudinal Slope - 4% Cross Slope	1.0	8.03	8.34	1.04	0.996	0.144	1.10
	2.0	16.06	16.31	2.03	1.035	0.183	2.00
	3.0	24.09	25.78	3.21	1.051	0.199	2.47
	4.0	32.12	32.71	4.07	1.055	0.203	2.59
	5.0	40.14	40.06	4.99	1.06	0.208	2.76
	6.0	48.17	48.42	6.03	1.067	0.215	3.00
	7.0	56.20	55.30	6.89	1.072	0.220	3.17
	8.0	64.23	64.74	8.06	1.078	0.226	3.39
	9.0	72.26	72.60	9.04	1.082	0.230	3.55
	10.0	80.29	80.76	10.06	1.085	0.233	3.66
	11.0	88.32	88.81	11.06	1.087	0.235	3.74
	12.0	96.35	96.41	12.01	1.090	0.238	3.86
- 5% Longitudinal Slope - 4% Cross Slope	1.0	8.03	8.70	1.08	0.999	0.147	1.16
	2.0	16.06	16.92	2.11	1.034	0.182	1.97
	3.0	24.09	23.96	2.98	1.043	0.191	2.23
	4.0	32.12	31.86	3.97	1.048	0.196	2.38
	5.0	40.14	41.01	5.11	1.058	0.206	2.69
	6.0	48.17	48.03	5.98	1.063	0.211	2.86
	7.0	56.20	56.45	7.03	1.069	0.217	3.07
	8.0	64.23	64.05	7.98	1.071	0.219	3.14
	9.0	72.26	72.96	9.09	1.073	0.221	3.21
	10.0	80.29	81.76	10.18	1.076	0.224	3.32
	11.0	88.32	88.56	11.03	1.077	0.225	3.36
	12.0	96.35	96.01	11.96	1.08	0.228	3.47

Table C: Numerical results of experiments (continued)

Configuration	Incoming gutter flow		Q Actual		Intercepted flow		
	Q _{Gutter} (cfs)	Q (gpm - m)		cfs	Pt Gage _{V-notch} (ft)	H _{V-notch} (ft)	Q _{CFI} (cfs)
-0.3% Longitudinal Slope - 2% Cross Slope	1.0	8.03	8.15	1.02	0.995	0.143	1.08
	2.0	16.06	16.32	2.03	1.031	0.179	1.89
	3.0	24.09	24.08	3.00	1.047	0.195	2.35
	4.0	32.12	32.30	4.02	1.057	0.205	2.66
	5.0	40.14	39.90	4.97	1.065	0.213	2.93
	6.0	48.17	48.50	6.04	1.074	0.222	3.25
	7.0	56.20	56.35	7.02	1.083	0.231	3.58
	8.0	64.23	63.60	7.92	1.09	0.238	3.86
	9.0	72.26	72.05	8.97	1.094	0.242	4.03
	10.0	80.29	80.60	10.04	1.1	0.248	4.28
	11.0	88.32	87.80	10.94	1.105	0.253	4.50
	12.0	96.35	96.10	11.97	1.107	0.255	4.59
- 1.0% Longitudinal Slope -2 % Cross Slope	1.0	8.03	8.46	1.05	0.994	0.142	1.06
	2.0	16.06	16.80	2.09	1.021	0.169	1.64
	3.0	24.09	24.20	3.01	1.038	0.186	2.09
	4.0	32.12	32.34	4.03	1.053	0.201	2.53
	5.0	40.14	40.50	5.04	1.057	0.205	2.66
	6.0	48.17	47.36	5.90	1.064	0.212	2.89
	7.0	56.20	56.70	7.06	1.073	0.221	3.21
	8.0	64.23	64.02	7.97	1.078	0.226	3.39
	9.0	72.26	72.80	9.07	1.082	0.230	3.55
	10.0	80.29	80.35	10.01	1.085	0.233	3.66
	11.0	88.32	88.30	11.00	1.089	0.237	3.82
	12.0	96.35	97.30	12.12	1.092	0.240	3.94

Table C: Numerical results of experiments (continued)

Configuration	Incoming gutter flow		Q Actual		Intercepted flow		
	Q _{Gutter} (cfs)	Q (gpm - m)		cfs	Pt Gage _{V-notch} (ft)	H _{V-notch} (ft)	Q _{CFI} (cfs)
- 1.5% Longitudinal Slope - 2% Cross Slope	1.0	8.03	8.22	1.02	0.992	0.140	1.02
	2.0	16.06	16.80	2.09	1.023	0.171	1.69
	3.0	24.09	23.80	2.96	1.031	0.179	1.89
	4.0	32.12	32.90	4.10	1.041	0.189	2.17
	5.0	40.14	40.45	5.04	1.048	0.196	2.38
	6.0	48.17	47.90	5.97	1.054	0.202	2.56
	7.0	56.20	56.00	6.97	1.061	0.209	2.79
	8.0	64.23	64.40	8.02	1.067	0.215	3.00
	9.0	72.26	73.20	9.12	1.068	0.216	3.03
	10.0	80.29	79.80	9.94	1.07	0.218	3.10
	11.0	88.32	88.40	11.01	1.072	0.220	3.17
	12.0	96.35	96.06	11.96	1.075	0.223	3.28
-3% Longitudinal Slope - 2% Cross Slope	1.0	8.03	8.40	1.05	0.996	0.144	1.10
	2.0	16.06	16.38	2.04	1.023	0.171	1.69
	3.0	24.09	24.86	3.10	1.035	0.183	2.00
	4.0	32.12	32.90	4.10	1.044	0.192	2.26
	5.0	40.14	39.00	4.86	1.046	0.194	2.32
	6.0	48.17	48.80	6.08	1.051	0.199	2.47
	7.0	56.20	56.00	6.97	1.054	0.202	2.56
	8.0	64.23	64.90	8.08	1.057	0.205	2.66
	9.0	72.26	71.95	8.96	1.06	0.208	2.76
	10.0	80.29	79.90	9.95	1.062	0.210	2.82
	11.0	88.32	87.60	10.91	1.066	0.214	2.96
	12.0	96.35	95.90	11.94	1.067	0.215	3.00

Table C: Numerical results of experiments (continued)

Configuration	Incoming gutter flow		Q _{Actual}		Intercepted flow		
	Q _{Gutter} (cfs)	Q (gpm - m)		cfs	Pt Gage _{V-notch} (ft)	H _{V-notch} (ft)	Q _{CFI} (cfs)
- 4% Longitudinal Slope - 2% Cross Slope	1.0	8.03	8.10	1.01	0.994	0.142	1.06
	2.0	16.06	16.44	2.05	1.015	0.163	1.50
	3.0	24.09	24.95	3.11	1.028	0.176	1.82
	4.0	32.12	32.55	4.05	1.035	0.183	2.00
	5.0	40.14	39.33	4.90	1.038	0.186	2.09
	6.0	48.17	48.10	5.99	1.045	0.193	2.29
	7.0	56.20	55.80	6.95	1.046	0.194	2.32
	8.0	64.23	64.35	8.01	1.052	0.200	2.50
	9.0	72.26	71.50	8.91	1.056	0.204	2.63
	10.0	80.29	80.20	9.99	1.059	0.207	2.72
	11.0	88.32	88.10	10.97	1.064	0.212	2.89
	12.0	96.35	96.50	12.02	1.066	0.214	2.96
- 5% Longitudinal Slope - 2% Cross Slope	1.0	8.03	8.65	1.08	0.994	0.142	1.06
	2.0	16.06	16.48	2.05	1.014	0.162	1.48
	3.0	24.09	24.38	3.04	1.027	0.175	1.79
	4.0	32.12	30.90	3.85	1.034	0.182	1.97
	5.0	40.14	41.00	5.11	1.04	0.188	2.14
	6.0	48.17	48.25	6.01	1.041	0.189	2.17
	7.0	56.20	56.20	7.00	1.047	0.195	2.35
	8.0	64.23	64.80	8.07	1.051	0.199	2.47
	9.0	72.26	72.15	8.99	1.055	0.203	2.59
	10.0	80.29	80.85	10.07	1.057	0.205	2.66
	11.0	88.32	88.40	11.01	1.058	0.206	2.69
	12.0	96.35	96.30	11.99	1.06	0.208	2.76